

# Exploring the plastivorous activity of *Hermetia illucens* (Diptera Stratiomyidae) larvae

Linda Abenaim<sup>1</sup>, David Mercati<sup>2</sup>, Alessandro Mandoli<sup>3</sup>, Joachim Carpentier<sup>4</sup>, Grégoire Noël<sup>4</sup>, Barbara Conti<sup>1\*</sup>, Rudy Caparros Megido<sup>4</sup>, Romano Dallai<sup>2</sup>

<sup>1</sup> Department of Agriculture, Food and Environment, University of Pisa, Via del Borghetto 80, 56126 Pisa, Italy

<sup>2</sup> Department of Life Science, University of Siena, Via Aldo Moro, 2, 53100 Siena, Italy

<sup>3</sup> Department of Chemistry and Industrial Chemistry, University of Pisa, Via Giuseppe Moruzzi, 13, 56124 Pisa, Italy

<sup>4</sup> Functional and Evolutionary Entomology, UR TERRA, Gembloux Agro-Bio Tech, University of Liège, Passage des Déportés 2, 5030 Gembloux, Belgique

\*Correspondence: [barbara.conti@unipi.it](mailto:barbara.conti@unipi.it)

## Abstract:

*Hermetia illucens* (Diptera Stratiomyidae), also known as Black Soldier Fly (BSF), is one of the insect species most investigated for biodegradation ability in its larvae. *H. illucens* larvae can biodegrade organic waste but also contaminants like pesticides, antibiotics, and mycotoxins. This study wants to investigate the ability of these larvae to degrade polystyrene (PS). Experiments evaluated the growth performance, survival rates, intestinal and intracellular morphological alterations, degradation by-product formation and intestinal microbiota alterations of larvae fed a PS-enriched diet. Despite the addition of PS microparticles, no significant differences in growth or survival were observed compared to the standard diet ( $p > 0.05$ ). Confocal Laser Scanning Microscopy and Transmission Electron Microscopy confirmed the presence of PS microparticles in the larval gut, with potential signs of biodegradation. Metabolomic analyses identified styrene in the gut after 1 and 3 days of PS feeding, but its occurrence was likely due to thermal depolymerisation of the PS microparticles under GC-MS conditions. Metagenomic analysis revealed significant shifts in the intestinal microbiota. Notably, an enrichment of *Corynebacterium*, known for its role in aerobic PS degradation, and the abundance increase of other genera (*Enterococcus*, *Enterobacteriaceae*, *Enterobacter*, and *Escherichia-Shigella*) associated with synthetic polymer metabolism was observed. These results confirm the potential of BSF larvae to manage plastic waste through the interaction between their gut microbiota and synthetic materials. This study provides a foundation for future research focusing on isolating bacterial communities and enzymatic processes involved in polymer degradation, aiming to develop sustainable strategies for plastic waste management.

**Keywords:** Black Soldier Fly, polystyrene, microparticles, biodegradation, intestinal microbiota, by-products

## 1. Introduction

In recent years, research has increasingly focused on the ability of specific insect species to biodegrade and bioconvert food waste into valuable resources, such as chitin, proteins, lipids, vitamins, and other compounds. Nevertheless, some insects can detoxify and biodegrade contaminants and xenobiotic substances, including pesticides, mycotoxins, and antibiotics (Carpentier et al., 2024). The bioconversion, degradation, and detoxification processes carried out by insects are strongly influenced by their associated microbial communities, which are shaped by the insects' diet. As these communities adapt to the specific substrates consumed, bacteria specialised in digesting those substrates gain a competitive advantage within the gastrointestinal tract (Engel & Moran, 2013; De Smet et al., 2018; Carpentier et al., 2024). This adaptation is significant when dealing with environmental contaminants, like plastic, one of the most widespread and hazardous pollutants. In 2022, global plastic production reached 400.3 million tonnes, further intensifying the ecological challenge of plastic recycling (Plastics Europe, 2024). Among the various types of plastics, polystyrene (PS) which consists of styrene monomers, is a widely used plastic in different industrial applications, including food packaging (Block et al., 2017), and is considered one of the most polluting synthetic polymers (Ullah et al., 2023).

48 In the past five years, the use of insects for the biodegradation of synthetic polymers has gained significant attention in  
49 scientific literature. However, insects do not biodegrade plastics independently; instead, they rely on intestinal  
50 microorganisms and their digestive enzymes for this process (Brandon et al., 2018; Bulak et al., 2018; Cucini et al., 2020;  
51 Jiang et al., 2021; Arunrattiyakorn et al., 2022). These microorganisms produce enzymes that break down plastic polymer  
52 chains into smaller molecules, such as multimers and dimers, which can be transformed into carbon dioxide, methane,  
53 and water, adsorbed by microbial cells and used as a carbon source to fuel their energy cycles (Danso et al., 2019; Othaman  
54 et al., 2021). While not all insect species can completely biodegrade synthetic polymers, some species have shown the  
55 capacity to ingest and degrade different synthetic polymers, including polyethylene (PE), polystyrene (PS), polypropylene  
56 (PP), and polyvinyl chloride (PVC). Among these “plastivorous” species there are *Tenebrio molitor* Linnaeus, 1758  
57 (Coleoptera Tenebrionidae), *Zophobas atratus* (Fabricius, 1775) (Coleoptera Tenebrionidae), *Alphitobius diaperinus*  
58 (Panzer, 1797) (Coleoptera Tenebrionidae), and *Galleria mellonella* (Linnaeus, 1758) (Lepidoptera Pyralidae) (Sanchez-  
59 Hernandez, 2021; Kuan et al., 2022; Pivato et al., 2022; Noël et al., 2023). Although lepidopterans and coleopterans have  
60 demonstrated this potential, other insect species may represent alternative options worth exploring. An example is  
61 *Hermetia illucens* (Linnaeus, 1758) (Diptera Stratiomyidae), known as Black Soldier Fly (BSF), one of the most  
62 investigated insect species for the ability of its larvae to consume and degrade a wide variety of organic substrates,  
63 including waste (Nyakeri et al., 2017; Amrul et al., 2022), and convert them into valuable resources (Kaczor et al., 2022).  
64 Besides, recent research highlighted the ability of BSF larvae to degrade and reduce contaminants like pesticides,  
65 antibiotics, and mycotoxins (Camenzuli et al., 2018; Liu et al., 2020; Mei et al., 2022; Suo et al., 2023). However, recent  
66 studies also showed the capability of BSF larvae to chew and ingest microplastics of PVC, PE, PS, PP and PA (polyamide)  
67 without any apparent negative effects on their performance and survival (Cho et al., 2020; Romano & Fisher, 2021;  
68 Lievens et al., 2022; Piersanti et al. 2024; Wang et al., 2024; Heussler et al., 2024).  
69 There is limited evidence that BSF larvae can degrade synthetic polymers, unlike other plastivorous insect species.  
70 Romano & Fisher (2021) found that BSF larvae exposed to PP microplastics exhibited high levels of propionic and butyric  
71 acid, which were absent in the larvae of the control diet. Since these short-chain fatty acids (SCFA) are of bacterial origin,  
72 their presence could be due to shifts in intestinal microbiota induced by the presence of plastic (Wang et al., 2021). Other  
73 authors observed changes in the intestinal microbiota of BSF larvae, suggesting a crucial role of the microbiota in  
74 degradation when exposed to plastic-contaminated diets (De Filippis et al., 2023, Piersanti et al. 2024; Wang et al., 2024;  
75 Heussler et al., 2024). However, there are only a few studies on plastic biodegradation by *H. illucens*, so further and more  
76 in-depth investigations are needed.  
77 This work aimed to investigate the ability of BSF larvae to consume and biodegrade a diet contaminated with PS  
78 microparticles. Using a multidisciplinary approach, we investigated the growth performance and survival rate of BSF  
79 larvae reared on the PS-contaminated substrate and the changes in the intestinal microbiota after administering a PS-  
80 contaminated diet.

## 81 **2. Materials and methods**

### 82 2.1. *Hermetia illucens* larval performance in a polystyrene-contaminated diet

83 Black Soldier Fly rearing is maintained under laboratory conditions (28 °C, 60% RH, and photoperiod 16:8 = L:D) at the  
84 Entomology Laboratory of the Department of Agriculture, Food and Environment at the University of Pisa since 2018  
85 (Adamaki-Sotiraki et al., 2024). Thirty 6-day-old larvae were used to assess BSF larval performance, with five replicates  
86 per diet (150 larvae total). The larvae were starved for 24 hours, weighed, and measured before being placed in a 330 mL  
87 glass container with 30 g of the total diet. Two diets were used: a standard diet (poultry feed – Micheletti and Zei SRL,

88 Italy – soaked in water at a 40:60 ratio) and a polystyrene-contaminated diet (poultry feed soaked in water in the same  
89 ratio, mixed with a 2% aqueous solution of fluorescent PS microparticles). Before adding the poultry feed, the PS  
90 microparticle solution was uniformly distributed in the water and extensively mixed into the feed to ensure homogeneous  
91 dispersion. The PS microparticles were purchased from Sigma Aldrich, Merck KGaA (St. Louis, Missouri, United States),  
92 commercialised as latex beads, carboxylate-modified polystyrene, fluorescent yellow-green, with a mean diameter of  
93 1.80-2.20  $\mu\text{m}$ , a fluorescence of  $\lambda_{\text{ex}}$  470 nm and  $\lambda_{\text{em}}$  505 nm, a density of 1.04-1.05  $\text{g}/\text{cm}^3$ , spherical shape and solid  
94 content in aqueous solution of 2.5% w/v. Given the use of 2% w/v aqueous PS solution with 2.5% w/v solid content, the  
95 total amount of solid PS in 30 g of diet was 15 mg, corresponding to a final concentration of 0.05% w/w (or 0.50 mg/g)  
96 of solid PS in the diet. Assuming a homogeneous distribution of PS in the food, each larva (30 larvae per diet) was  
97 estimated to ingest approximately 0.50 mg of PS microparticles, a concentration similar to that tested in previous studies  
98 (Lou et al., 2020; Wang et al., 2022). The microplastic concentration used in the present paper also falls within the range  
99 of microplastic levels in contaminated soil (0.03-6.7% w/w) and organic and food waste (0.001-5.6% w/w), as reported  
100 by Fuller and Gautam (2016) and Porterfield et al. (2023), which BSF larvae may naturally come into contact with.  
101 The entire experiment, including five replicates per diet (150 larvae in total per diet), was repeated in three independent  
102 trials. Larval performances were assessed by recording survival rate (%), weight, and length every three days until the  
103 pupation. The weight and length of the larvae were measured when mature (15 days old). The individual weight of the  
104 larvae was assessed using an analytical balance, and their length was measured with a ruler. The larval survival rate (%)  
105 was calculated using the following formula:

$$106 \text{ Larval survival rate (\%)} = \frac{\text{Final number of larvae}}{\text{Initial number of larvae}} \times 100$$

107 Before measurement, all larvae were rinsed with water and thoroughly dried with absorbent paper before weighing. As  
108 soon as prepupae were obtained, they were placed in a new box to allow pupation and track their survival and adult  
109 emergence.

## 111 2.2. Ultrastructural observations of *Hermetia illucens* larval gut

112 Ultrastructural observations of the larval gut were conducted using a Confocal Laser Scanning Microscope (CLSM; Zeiss  
113 LSM 700) at the Department of Life Sciences, University of Siena to assess the presence of PS in the larval gut and any  
114 morphological alterations. The observations were conducted on a total of 10 mature larvae, 5 treated and 5 control larvae  
115 of 15 days old, fed on the PS diet and standard diet respectively. Guts were dissected in sterile 0.1 M phosphate buffer  
116 (pH 7.2), to which 3% of sucrose was previously added (PB), under a stereomicroscope. Transmission Electron  
117 Microscopy (TEM) observations were performed to detect any intracellular differences between the midgut epithelium  
118 of larvae reared on the standard diet and those on the PS diet. The larval midgut epithelium was dissected and fixed at 4  
119  $^{\circ}\text{C}$  in both treatments with 2.5% glutaraldehyde in PB. After 24 hours, each sample was rinsed in buffer and post-fixed in  
120 1% osmium tetroxide for 1 hour at 4  $^{\circ}\text{C}$ . After dehydration in ethanol, the samples were incorporated in a mix of Epon-  
121 Araldite. Ultrathin sections of each sample were obtained with a Reichert Ultracut II E ultramicrotome, routinely stained  
122 with uranyl acetate and lead citrate, and then observed in a TEM Philips CM10 operating at an electron accelerating  
123 voltage of 80 kV.

## 125 2.3. Metabolomic analysis

126 To detect PS degradation products, 150 six-day-old larvae (divided into three replicates of 50 larvae each) were fed 50 g  
127 of the PS-based diet or 50 g of the standard diet. To assess the presence of PS degradation products, all larvae for each  
128 diet were collected after 1, 3, and 7 days, thoroughly washed, dried, and stored at -20  $^{\circ}\text{C}$ . Analytical samples for GC-MS

129 analysis were prepared according to Tsochatzi et al. (2021), by blending the larvae for 2 minutes with a domestic grinder  
130 and then subjecting them to lyophilisation (LIO 5PDGT, 5PASCAL) at -20 °C and 1030 mbar. After 24 hours of  
131 lyophilisation, the powder samples were stored at -20 °C until analysis. The extraction and GC-MS analyses were carried  
132 out at the Department of Chemistry and Industrial Chemistry at the University of Pisa. For the extraction, a lyophilised  
133 sample of 0.3-0.5 g was placed in a glass tube with 2.0 mL of dichloromethane (DCM). The tube was vortexed for 1  
134 minute, sonicated for 1 hour at 25 °C, and centrifugated at 2500 rpm for 5 minutes at room temperature. The supernatant  
135 was filtered through a 0.2 mm PTFE (polytetrafluoroethylene) membrane and the clear filtrate was immediately subjected  
136 to analysis with a Varian 3800 GC coupled to a Saturn 2000 ion trap. The working conditions were: J&W DB-1MS column  
137 (30 m × 0.25 mm × 0.25 mm), 1.0 mL min<sup>-1</sup> helium flow rate, splitless injection mode at 300 °C, with a purge flow of 1.5  
138 minutes. The oven program started at 40 °C for 10 minutes, followed by a linear temperature ramp at 30 °C min<sup>-1</sup> up to  
139 320 °C. The electron ionization (EI<sup>+</sup>) spectra were acquired in the 55-350 *m/z* range in either the MS or MS/MS mode.  
140 Standard solutions of styrene (ST), *a*-methylstyrene (aMS), acetophenone (ACP), and cumyl alcohol (CA) in DCM (2-  
141 1000 ppb) were injected to determine the retention time and limit of detection (LOD) of each of the analyte reported by  
142 Tsochatzi et al. (2021).

143

#### 144 2.4. Metagenomic analysis

##### 145 *Samples preparation and DNA extraction*

146 DNA was extracted from the gut contents of 12 mature larvae (15 days old) per diet group (PS treated and control) for a  
147 total of 24 larvae at the Gembloux Agro-Bio Tech Department, University of Liège (Belgium). Before DNA extraction,  
148 the larvae were washed using distilled water and 70% ethanol for 10 minutes, followed by a triple rinse in distilled water.  
149 The specimens were killed in liquid nitrogen and dissected in an iced Petri dish with paraffin filled with PBS, to maintain  
150 cold conditions during the dissection and avoid degradation. Then, the entire gut dissected and extracted was placed into  
151 a sterile 1.5 mL Eppendorf and cryopreserved by directly plunging into liquid nitrogen, and the samples were kept at -80  
152 °C. The RETSCH Mixer mill pulveriser was used to disaggregate the samples. The DNA was extracted using the Qiagen  
153 QIAamp PowerFecal Pro DNA Kit protocol, according to the manufacturer's instructions (ID: 51804, Qiagen, Hilden,  
154 Germany). The DNA quality was checked using a Nanodrop ND-1000 spectrophotometer (NanoDrop Technologies,  
155 Wilmington, DE, USA). Qubit 1.0 (dsDNA quantitative analysis kit, Invitrogen, Carlsbad, CA, USA) was used to quantify  
156 the amount of DNA. The DNA integrity was evaluated by agarose gel electrophoresis (2%). The extracted DNA samples  
157 were stored at -20 °C until amplification.

158

##### 159 *16S rRNA gene amplification by Polymerase Chain Reaction*

160 Polymerase chain reaction (PCR) amplification was performed on the V3-V4 hypervariable region of the 16S rRNA gene  
161 using primers pair S-D-Bact-0341-b-S-17 (5'-CCTACGGGNGGCWGCAG-3') and S-D-Bact-0785-a-A-21 (5'-  
162 GACTACHVGGGTATCTAATC-3') (Klindworth et al., 2013). All PCR reactions were performed in a volume of 50 µl  
163 containing 2 µl of BSF samples DNA, 1.5 µL of each primer at 1 µM, 20 µl of H<sub>2</sub>O, and 25 µl of 2x KAPA Hifi HotStart  
164 Ready Mix (KAPA Biosystems, Wilmington, MA, USA). The PCR was carried out in a thermocycler by using the  
165 following cycle: 95 °C for 3 minutes, 98 °C for 20 seconds, 60 °C for 15 seconds, 72 °C for 30 seconds, 72 °C for 1  
166 minute. The cycle was repeated 30 times. For quality control, 5 µL of PCR products were loaded in 2% electrophoresis  
167 gel and visualised under UV light to check if the expected band was obtained. The amplified products were purified using  
168 the NucleoSpin Gel and PCR Clean-up system (Macherey-Nagel, Düren, Germany). Then, the DNA amplicons were  
169 stored at 4 °C.

170

### 171 *Gene library preparation and sequencing of the 16S rRNA*

172 The PCR products were sent to the Institute of Biotechnology at Cornell University (Ithaca, NY, USA) for 16S library  
173 preparation and Illumina sequencing processing. Briefly, PCR products underwent purification through a PCR clean-up  
174 protocol which included the AMPure XP beads system (Beckman Coulter, Brea, CA, USA). Next, the NEXTERA XT  
175 Index Kit (Illumina, San Diego, USA) was utilised to affix dual indices and Illumina sequencing adapters for all the  
176 samples. DNA samples were standardised to a concentration of 4 nM and subsequently processed for sequencing in  
177 alignment with the Illumina system Denature and Dilute Libraries Guide. The MiSeq Illumina system was used for  
178 processing paired-end sequencing (2x250 bp).

179

### 180 *Bioinformatics analyses*

181 Subsequent demultiplexed raw sequences were processed using QIIME2 software (Quantitative Insights Into Microbial  
182 Ecology, version 2023.2) (Bolyen et al. 2019). Illumina Miseq sequencing of the V3-V4 region of the 16S rRNA gene  
183 generated a total of 2,430,269 reads (for both forward sequence count and reverse sequence count) across 12 samples  
184 from both, from a maximum of 147,091 to a minimum of 2,956, with an average of  $101,261 \pm 35,628$  unpaired sequences  
185 per sample. The primers were trimmed with the plug-in cutadapt (Martin, 2011). After the reads were filtered on quality,  
186 denoised and merged with the DADA2 plug-in (Callahan et al., 2016) with --p-trunc-len-f 220, --p-trunc-len-r 220, --p-  
187 trim-left-f 18, --p-trim-left-r 21, resulting in high resolution of ASVs for downstream assessment. After filtering,  $68,923$   
188  $\pm 26,151$  unique sequences were conserved for the taxonomic assignment. The plug-in q2-feature-classifier (Bokulich et  
189 al., 2018) was used for the taxonomy assignment using a Naive Bayes classifier trained on the V3-V4 region of the target  
190 sequences and SILVA 138 reference database with a 99% similarity threshold (Robeson et al., 2021). Mitochondria and  
191 chloroplasts were excluded from the resulting ASVs table and then analysed using RStudio software (version 4.3.2) to  
192 visualise the different taxonomy between the two diets. To control for possible bias introduced by contaminants in our  
193 analyses, a filtering threshold of 1% for low abundant ASVs and additional filtering of ASVs present in less than 20% of  
194 samples were applied. The diversity analyses were measured with a q2-diversity plug-in following the core-metrics-  
195 phylogenetic method. In particular, the alpha diversity was based on the Faith Phylogenetic Diversity (Faith-pd) and  
196 Pielou-evenness metrics. The beta diversity was based on the Jaccard distance matrix and visualised with PCoA. The  
197 group significance between beta diversity was analysed using Permutational Multivariate Analysis of Variance  
198 (PERMANOVA). ASVs differentially abundant across groups were identified at genus and family levels with bias-  
199 corrected microbiome composition analysis (ANCOM-BC) (Lin & Peddada, 2020). Bacterial species with more than 1%  
200 relative abundance were included in this analysis to detect major species variations. Subsequently, the da-barplot was  
201 used to visualise the output of ANCOM-BC represented by the model Log Fold Change (LFC) which describes how much  
202 a quantity changes between an original and a subsequent measurement. The significance threshold, effect size threshold,  
203 and feature IDs were used to filter the results. Only the ASVs that passed all three filters were included in the output.

204

### 205 2.5. Statistical analysis

206 Larval growth performance (larval weight and length) was statistically compared between diets using the t-Student test  
207 ( $p < 0.05$ ) (JMP software, JMP®, Version 16. SAS Institute Inc., Cary, NC, 1989–2021). Alpha diversity of the microbiome  
208 data was assessed with the Kruskal-Wallis test followed by the Wilcoxon rank-sum test ( $p < 0.05$ ). Beta differences in  
209 overall microbiome taxonomic composition by diet were analysed using PERMANOVA on the Jaccard distance ( $p < 0.05$ ).

210 Differential abundance was evaluated with the FDR method (False Discovery Rate) incorporated in the ANCOM-BC with  
211 the Bonferroni method ( $p < 0.05$ ).

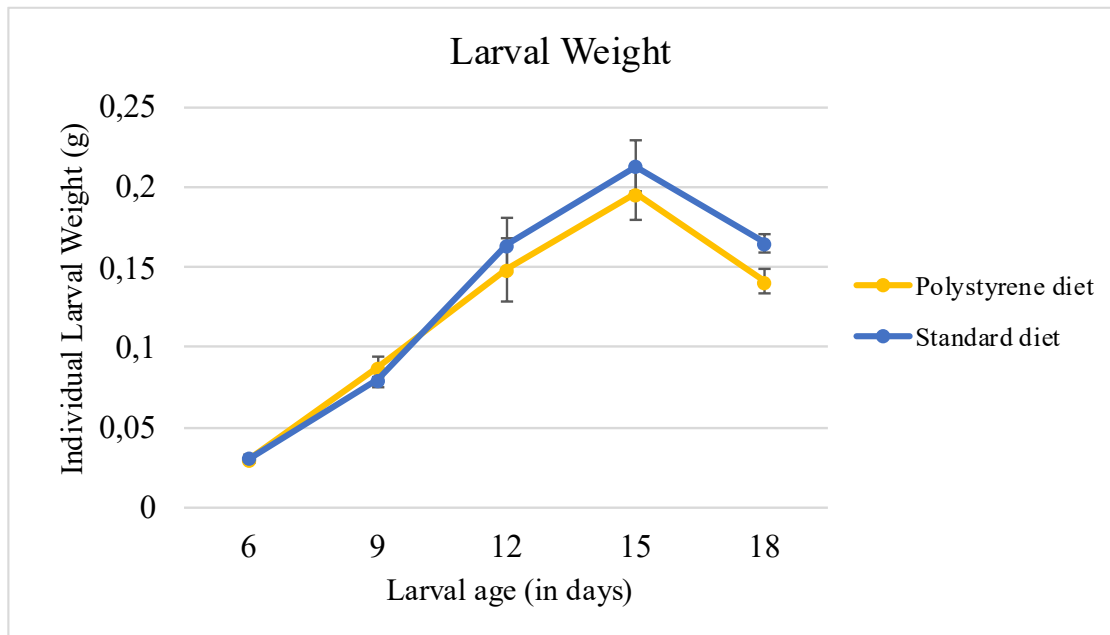
212

### 213 3. Results and Discussion

#### 214 3.1. *Hermetia illucens* development in a polystyrene-contaminated diet

215 The weight and length of the larvae reared on the two different diets were checked every three days until all larvae were  
216 moulted in prepupae (18 days old). However, the comparison was made based on the larval performance shown in a  
217 previous paper (Adamaki-Sotiraki et al., 2024), when they were 15 days old (mature larvae), and their weight was  
218 maximum. At this time, in fact, the mature larvae stopped feeding to prepare for the moult and their weight decreased  
219 from then on (Figures 1 and 2).

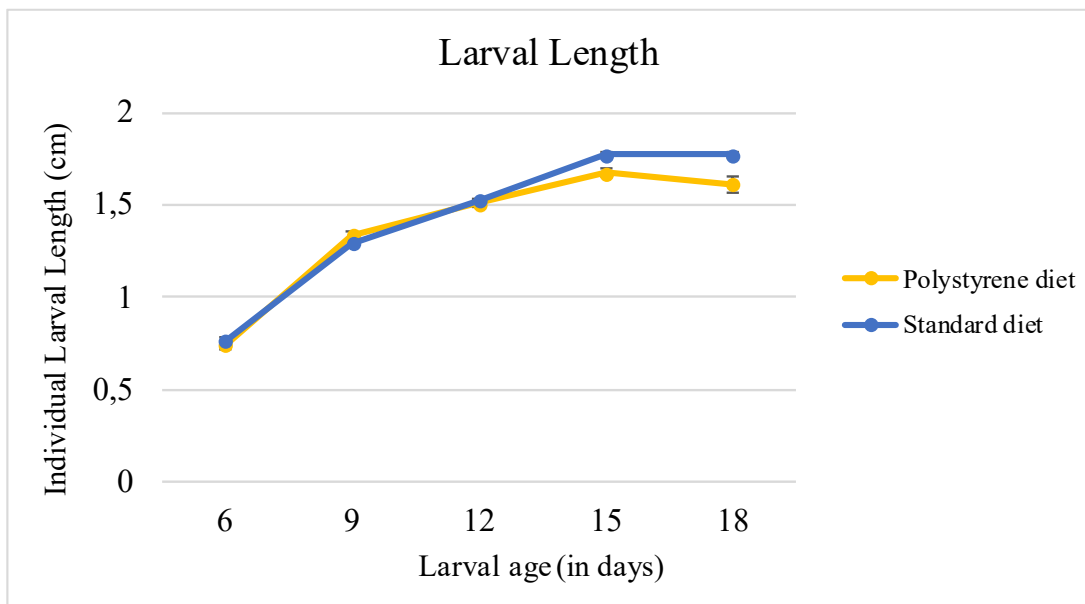
220



221

222 **Figure 1.** The average individual weight of *Hermetia illucens* larvae fed on the standard and polystyrene diet. A group of  
223 30 larvae were tested, and 5 replicates for each diet were performed for 150 larvae/diet.

224



225

226 **Figure 2.** The average individual length of *Hermetia illucens* larvae fed on the standard and polystyrene diet. A group of  
227 30 larvae were tested, and 5 replicates for each diet were performed for 150 larvae/diet.  
228

229 The t-Student test did not show significant differences between the two diet treatments regarding individual larval weight  
230 and length ( $t = 2.306$ ;  $p = 0.528$  and  $t = 2.306$ ;  $p = 0.676$ , for larval weight and length, respectively). The average individual  
231 larval weight was  $0.190 \pm 0.008$  g for the PS diet and  $0.210 \pm 0.006$  g for the standard diet. The average individual larval  
232 length was  $1.670 \pm 0.02$  cm and  $1.770 \pm 0.01$  cm for PS and standard diet, respectively.

233 No significant differences in larval survival rates (%) were observed between the two diets. Both groups of larvae  
234 exhibited high survival rates, with  $98.8 \pm 0.6\%$  and  $99.3 \pm 0.6\%$  for polystyrene and standard diets, respectively.

235 These results are consistent with previous research on the larval performance of plastivorous insects, such as *T. molitor*,  
236 *G. mellonella*, and *Z. atratus*, reared on the PS diet (Peng et al., 2020; Lou et al., 2020; Matyja et al., 2020; Yang et al.,  
237 2020; Quan et al., 2023). Similar outcomes have been reported when PS was supplied as the sole nutritional source (Peng  
238 et al., 2022; Jiang et al., 2021; Yang et al., 2020) and when PS was incorporated into the diet. Similarly to our study, PS  
239 added to bran did not affect the survival of *Z. atratus* larvae, which was approximately 94-95% with no significant  
240 differences compared to the control diet consisting of only bran (Peng et al., 2020). Our results also agree with studies on  
241 *G. mellonella* and *T. molitor* (Lou et al., 2020; Matyja et al., 2020). PS added to beeswax and bran diets showed no  
242 statistically significant differences in *G. mellonella* larval development when compared to control diets, while *T. molitor*  
243 larvae fed with PS added to the oats diet exhibited high survival rates (approximately 90%), with no significant differences  
244 compared to the corresponding control diet. However, in the studies previously described, plastic was provided in its  
245 original form, as the larval stages of the species used all possess mandibular mouthparts capable of chewing and ingesting  
246 plastic in this form.

247 The same type of microparticles used in the present study was also employed in other research, in which insect  
248 performances were assessed, even if in lower concentrations (Muhammad et al., 2021; Wang et al., 2021; El Kholy & Al  
249 Naggari, 2023). In particular, in *Bombyx mori* (Linnaeus, 1758) (Lepidoptera Bombycidae) larvae the exposition to PS  
250 microparticle in 10  $\mu\text{g}/\text{mL}$  concentration (5–5.9  $\mu\text{m}$  diameter) showed no significant changes in body mass or survival  
251 compared to the control group (Muhammad et al., 2021). In *Apis mellifera* (Linnaeus, 1758) (Hymenoptera Apidae),  
252 exposure to PS microparticles at concentrations of 0.5, 5 and 50  $\text{mg}/\text{L}$  (25  $\mu\text{m}$  diameter) resulted in only a small effect on  
253 mortality (from 1.43 to 1.6%), with no statistical difference in body weight compared to the control diet (Wang et al.,  
254 2021). In contrast, *Drosophila melanogaster* Meigen, 1830 (Diptera Drosophilidae) exposed to three different  
255 concentrations of PS microparticles (1.8-2.20  $\mu\text{m}$  diameter), 0.005, 0.05 and 0.5  $\mu\text{g}/\text{ml}$ , showed a significant reduction in  
256 survival compared to the control diet (El Kholy & Al Naggari, 2023).

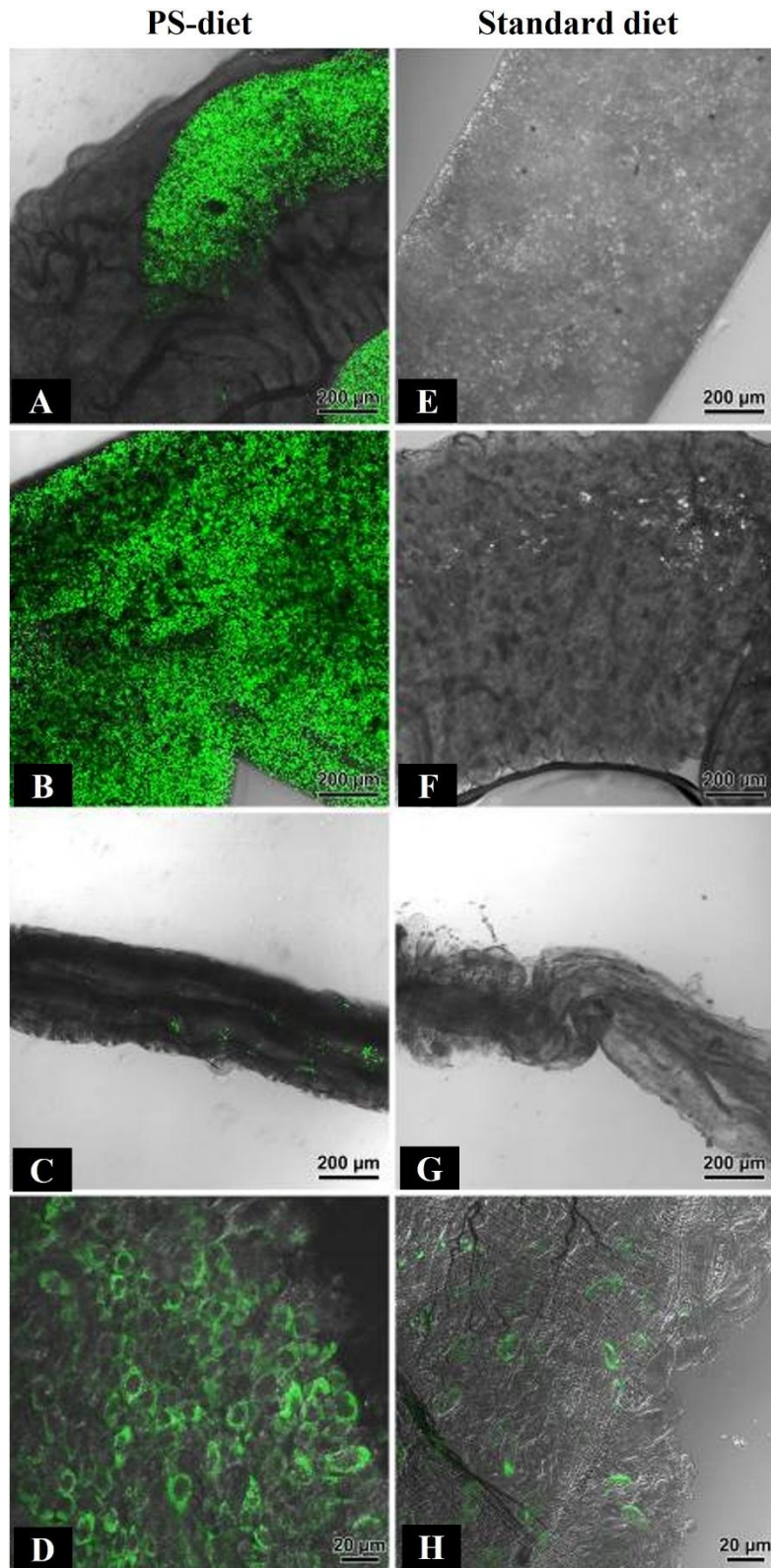
257 In the case of BSF, our findings align with those of Cho et al. (2020), who reported no significant differences in larval  
258 weight between PS-contaminated and control diets, although the PS concentration in the treated diet was higher than in  
259 the present study (50, 100 and 200  $\text{mg}/\text{g}$ ). Once larvae were mature (15 days old), the average larval weight in their study  
260 was 0.2 g for both diets, which aligns closely with our results ( $0.190 \pm 0.008$  g and  $0.210 \pm 0.006$  g, respectively for PS-  
261 contaminated and control diet). Moreover, the survival percentage for both diets was about 95%, like our results ( $98.8 \pm$   
262  $0.6\%$  and  $99.3 \pm 0.6\%$ , for PS and control diets, respectively). Besides PS, other synthetic polymers, such as PVC, PP and  
263 PE were also evaluated in the larval diet for BSF. Lievens et al. (2022) found no significant differences in weight (0.2 g)  
264 or survival rates (90%) between PVC-based (10  $\text{mg}/\text{g}$ ) and control diets, in line with our findings. Similarly, Romano and  
265 Fisher (2021) reported high larval survival (81%) with a PP-based diet, with no substantial differences compared to control  
266 diets, even though the concentration of microparticles in the treated diet was lower than the one in the present work (0.022  
267  $\text{mg}/\text{g}$ ). Cho et al., (2020) also reported that BSF larvae reared on PE-based diet showed no significant differences in

268 survival rate or mean larval weight compared to the controls at all tested concentration (50, 100 and 200 mg/g). Our study  
269 confirms that including PS in the diet does not adversely affect BSF larval growth or survival. The data indicate that BSF  
270 larvae can grow similarly in environments contaminated with plastic. This capability is shared by other plastivorous  
271 species (*T. molitor*, *G. mellonella*, *Z. atratus*), further highlighting the potential of these organisms in bioconversion and  
272 plastic degradation research (Peng et al., 2020; Pena-Pascagaza et al., 2020).

273

### 274 3.2. Evidence of plastic presence in the larval gut

275 Confocal Laser Scanning Microscope (CLSM) observations of the guts of BSF mature larvae (15 days old) reared on the  
276 PS diet revealed the presence of fluorescent PS-microparticles inside the gut lumen (**Figure 3**), confirming the ingestion  
277 of food combined with the plastic particles.



278

279 **Figure 3.** Confocal Laser Scanning Microscope observations of Black Soldier Fly larval gut. A-E) the foregut of larvae  
 280 reared on both polystyrene diet and standard diet; B-F) the midgut of both treatments; C-G) the hindgut of both treatments;  
 281 D-H) provides a detailed view of the midgut epithelium of larvae reared on both polystyrene diet (D) and standard diet  
 282 (H).

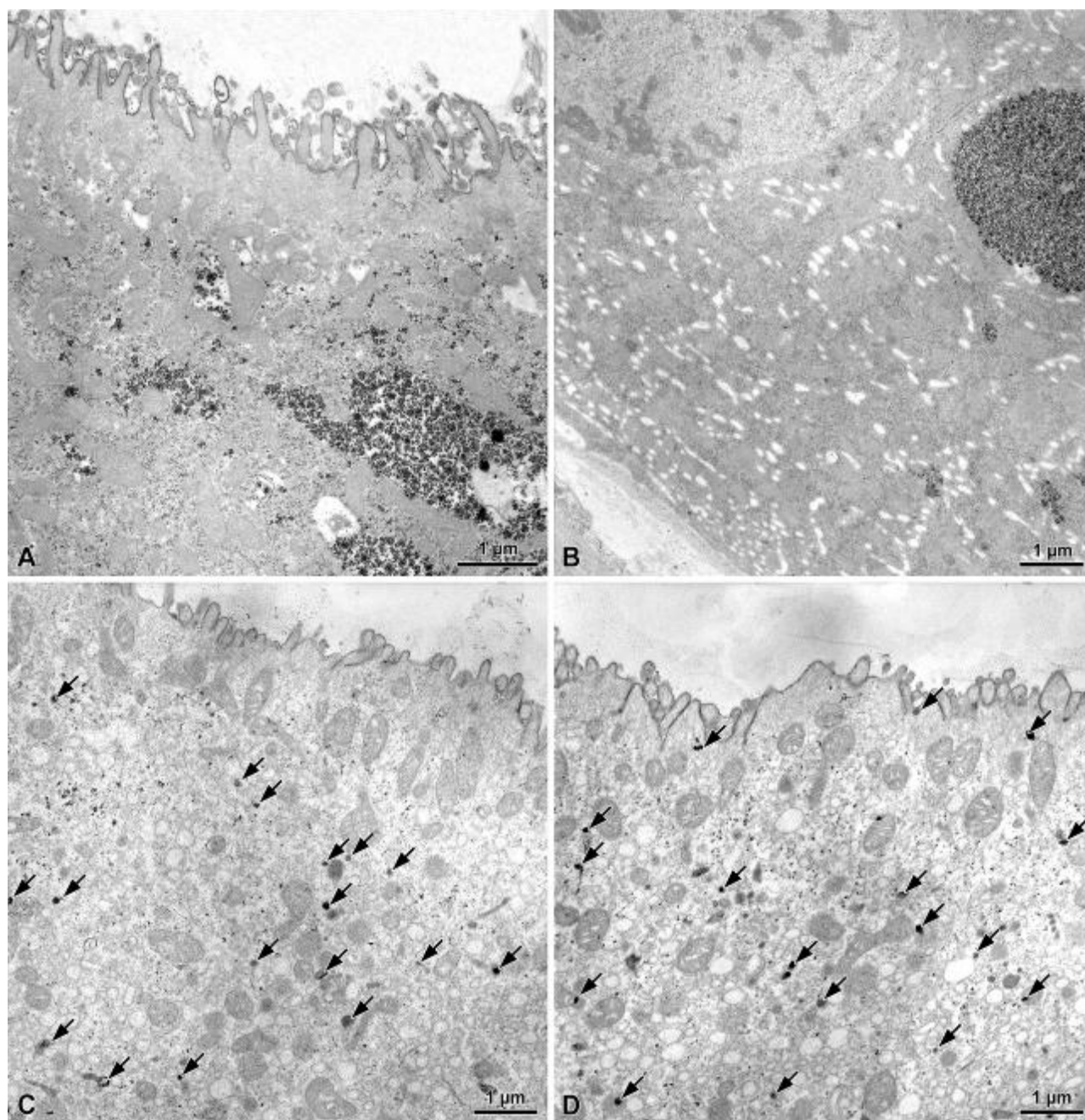
283

284

285 The findings indicate that the foregut and midgut of BSF larvae fed a PS diet contained a high concentration of fluorescent  
 286 PS microparticles (**Figure 3 A, B**). In contrast, the hindgut showed a significantly lower presence of PS microparticles,

287 as evidenced by the low fluorescence intensity (**Figure 3 C**). This latter effect may be related to the degradation of PS  
288 microparticles in the midgut due to the action of intestinal microbiota, as suggested by previous studies (Bruno et al.,  
289 2019). The midgut epithelial cells also exhibited strong fluorescence (**Figure 3 D**), implying that degraded PS fragments  
290 could have been transported across cells as metabolites or by-products of polymer degradation. Conversely, no  
291 fluorescence was detected along the gut of larvae fed the control diet (**Figure 3 E, F, G**). Nonetheless, some weak natural  
292 fluorescence was observed in the epithelial cells of the midgut of control-fed larvae, although with much lower intensity  
293 than the cells of larvae on the PS diet (**Figure 3 H**). This fluorescence is likely due to the intrinsic autofluorescence of  
294 the cells mainly originated from mitochondria and lysosomes, as described in prior studies (Monici, 2005; Koga et al.,  
295 2009). To further investigate the presence of PS microparticles at the cellular level, the midgut epithelium of BSF larvae  
296 reared on both diets was examined using TEM (**Figure 4**).

297



298

299 **Figure 4.** Transmission electron microscopy observations of the midgut epithelium of Black Soldier Fly larval gut. A)  
300 and B) Cross-sections of the midgut epithelium of larvae reared on the standard diet. C) and D) Cross-sections of the  
301 midgut epithelium of larvae reared on a diet contaminated with polystyrene. The arrows indicate the presence of numerous  
302 dense formations of approximately 50 nm in the epithelial cells, which are not present in those of larvae reared on the  
303 control diet.  
304

305 TEM observations revealed that the midgut epithelium is characterised by cells approximately 20  $\mu\text{m}$  in height. The cells  
306 of the midgut epithelium of larvae reared on the PS and control diets have a basal lamina thick 0.5-0.6  $\mu\text{m}$  and a basal  
307 nucleus of approximately 2.3  $\mu\text{m}$  in diameter. The basal region of the cells contains a series of deep invaginations of the  
308 plasma membrane, forming chains of small extracellular cavities that reach up to about half the height of the cell. In the  
309 apical region, the cells are separated by tortuous invaginations protruding into the cytoplasm, while the apex is bordered  
310 by a thin layer of microvilli about 0.6  $\mu\text{m}$  high.

311 In the cells of insects reared on the control diet, numerous glycogen granules are visible in the apical and median regions,  
312 often compacted to form large clusters. In the cells of insects reared on the control PS diet, glycogen clusters are also  
313 observed, although they appear less thick. Dense formations of approximately 80-150 nm in diameter were detected in  
314 the apical region of the cells, just below the zone with microvilli. These formations were absent in the control and may  
315 be attributed to material derived from the degradation of PS.

316 Despite these formations, the morphology of the midgut epithelium in larvae exposed to the PS diet did not display  
317 significant alterations or detectable differences compared to those of the standard diet, following the results of Piersanti  
318 et al. (2024).

319 Confocal Laser Scanning Microscope investigations showed a high concentration of PS microparticles in the foregut and  
320 midgut, with fewer in the hindgut, suggesting potential biodegradation. Neither CLSM nor TEM revealed significant  
321 structural alterations in the larval intestine of BSF exposed to PS microparticles.

322 Previous studies by Wang et al. (2022) used fluorescently labelled PS microparticles to track their presence within the  
323 entire intestine of *G. mellonella* larvae. They reported a decrease in fluorescence over time (after 3, 6, 12 and 18h of 27,  
324 56, 66, and 80%, respectively), suggesting the intestinal bacteria's potential depolymerisation and fragmentation of PS.

325 On the other hand, our TEM observations identified small, undefined dense aggregates in the midgut epithelial cells.  
326 Similarly, Wang et al. (2021) and Wang et al. (2022) observed similar formation via SEM in the midgut of *G. mellonella*  
327 and *A. mellifera*. These formations were linked to plastic particles, often accompanied by bacteria colonisation, indicating  
328 microbial degradation of plastics. For *G. mellonella*, PS particles in the midgut assumed irregular and smaller shapes after  
329 6 hours from ingestion and were degraded entirely after 24 hours (Wang et al., 2022).

330 Our study's dense granules discovered in the epithelial cells likely represent by-products of PS decomposition and  
331 digestion. This hypothesis aligns with the findings by Elmekawy et al. (2023), who described similar formations in the  
332 epithelial cells of *G. mellonella* after exposure to low-density PE. Additional support comes from CLSM analysis, which  
333 revealed a high fluorescence level in the midgut epithelium. While commercially produced by an unspecified process, the  
334 fluorescent PS microparticles used in this study, likely contain fluorophores resistant to enzymatic attack and capable of  
335 intracellular transport (Prabhakar et al., 2020).

336

### 337 3.3. Evaluation of polystyrene biodegradation products

338 Previous work (Tsochatzis et al., 2020) identified DCM as a suitable solvent for extracting PS and its degradation products  
339 (monomers, oligomers, and oxygenated derivatives) from *T. molitor* larvae, thereby leading to the GC-MS identification  
340 of ST, aMS, ACP, CA, and a few ST oligomers as competent markers of PS biodegradation.

341 At variance with the literature investigation, in our study, GC-MS evidence could be gained only for the ST monomer  
342 (**Figure S1 a, b**) and just for the extracts of the larvae taken at one and three days. In this regard, it must be pointed out,  
343 however, that the injection of a diluted solution of PS latex in DCM also led to the ST peak being clearly observed in the  
344 chromatogram. This latter result is likely due to the thermal depolymerisation of PS in the hot GC-MS injection port (see  
345 for instance Yang et al. 2020), which makes ST ill-suited to assess biodegradation of the polymer material by this  
346 analytical technique.

347 Therefore, even if multiple studies have identified ST as the primary product in the early stages of microbial PS  
348 degradation (Othman et al., 2021; Tsochatzis et al., 2021; Wang et al., 2022), no definitive conclusion about this aspect  
349 can be drawn herein.

350 Moreover, the lack of observing the other low-molecular-weight substances noted above (aMS, ACP, CA) could reflect  
351 the occurrence of different biodegradation pathways depending on the microbial community involved (Warhurst &  
352 Fewson, 1994; O’Leary et al., 2002; Ho et al., 2018; Ru et al., 2020; Hou & Majumder, 2021; Wang et al., 2022).

353 However, it is worth pointing out that ST was detected only in larvae extracts at days 1 and 3 and was absent after 7 days  
354 (**Figure S2**). Although ST alone cannot be reliably used as a marker of PS degradation due to potential artefacts, its  
355 disappearance over time may suggest that the monomer and potentially other degradation products were metabolised or  
356 eliminate by the larvae .

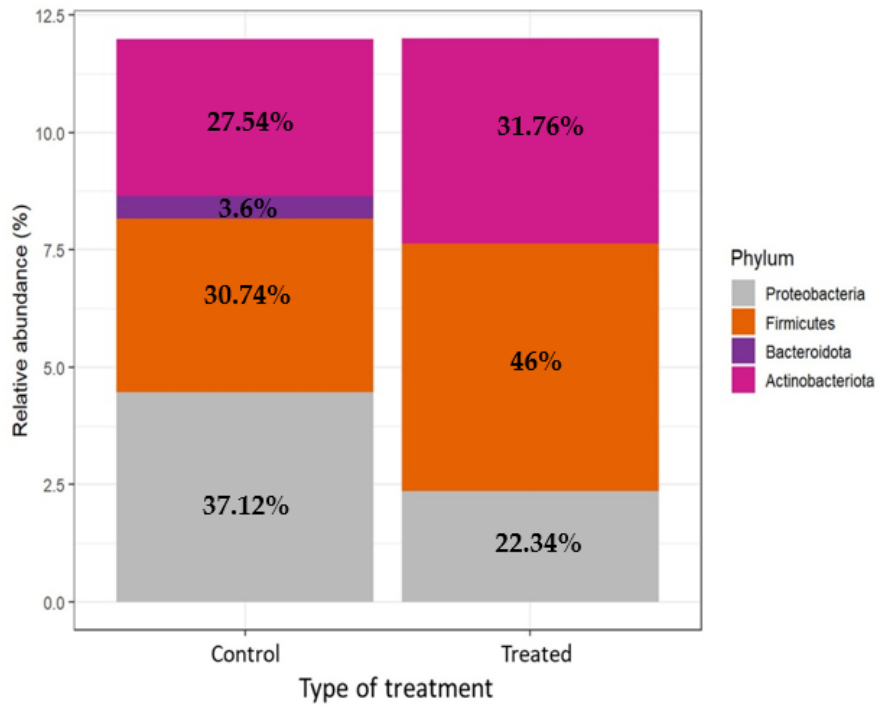
357

#### 358 3.4. Identification of polystyrene degradation microbial community

359 Microbial diversities were analysed in both experimental treatments after removing low-abundant ASVs (< 1%) in less  
360 than 20% of the samples. Following the filters, the number of ASVs decreased from 810 to 138. From the clustering of  
361 reads into ASVs and the annotation using the SILVA 138 database, Proteobacteria, Firmicutes, and Actinobacteriota were  
362 the main phyla observed for both treatments, representing 37.12 and 22.34%, 30.74 and 46%, and 27.54 and 31.76% for  
363 control and treated diet respectively (**Figure 5 a**). Additionally, the phylum Bacteroidota was found in small quantities in  
364 the gut microbiota of larvae reared on control diets (3.6%). **Figure 5 b** shows the average relative abundance of families  
365 represented by more than 1%. The most abundant families were Actinomycetaceae (31 and 29%), Enterococcaceae (16.4  
366 and 38%), Morganellaceae (35.5 and 18%), Lactobacillaceae (9.4 and 6%), regardless of the treatment, and  
367 Corynebacteriaceae 5.7% only in the treated diet. Similarly, the most abundant genera were *Actinomyces* (31 and 29%),  
368 *Enterococcus* (16.4 and 38%), *Morganella* (25.5 and 8.5%), *Providencia* (10 and 9.3%), *Lactobacillus* (9.4 and 6%), and  
369 *Corynebacterium* (5.7% only in the treated diet) (**Figure 5 c**).

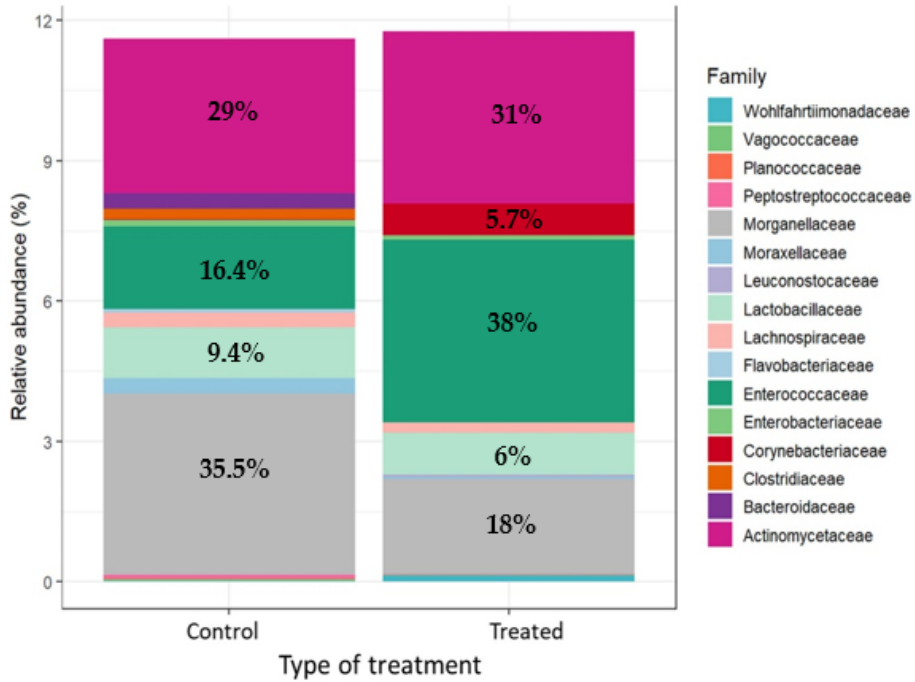
370

a) Phylum level of BSF bacterial community according to the diet (relative abundance >1%)



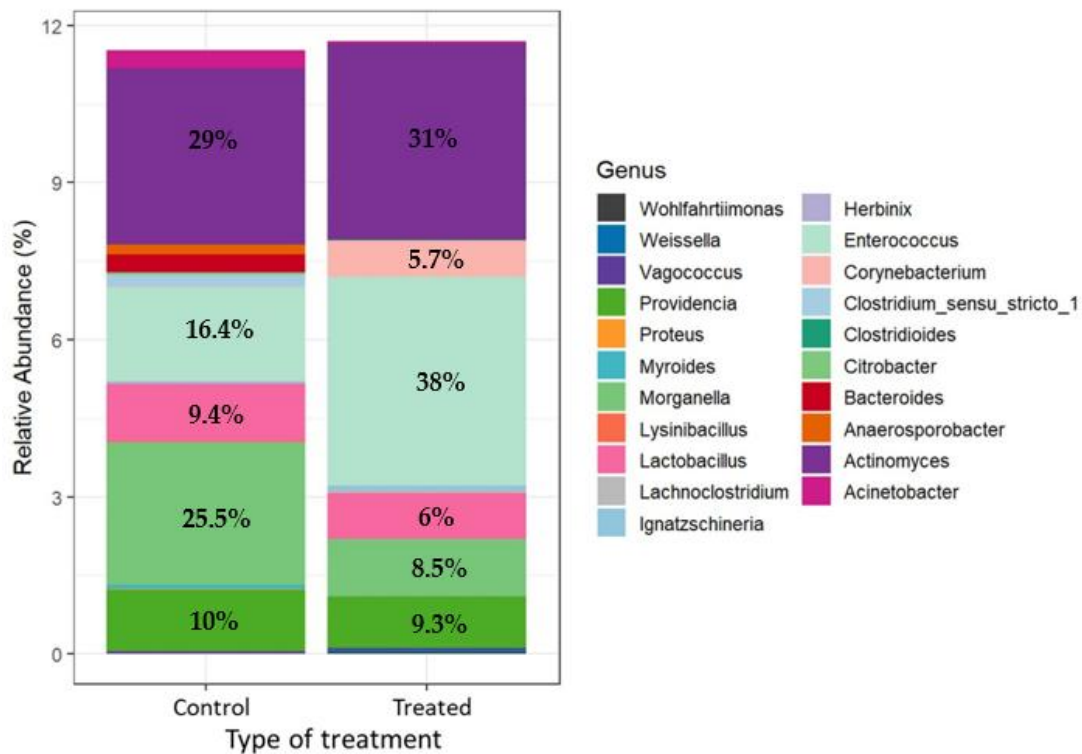
371  
372  
373

b) Family level of BSF bacterial community according to the diet (relative abundance >1%)



374

c) Genus level of BSF bacterial community according to the diet  
(relative abundance >1%)



375

376

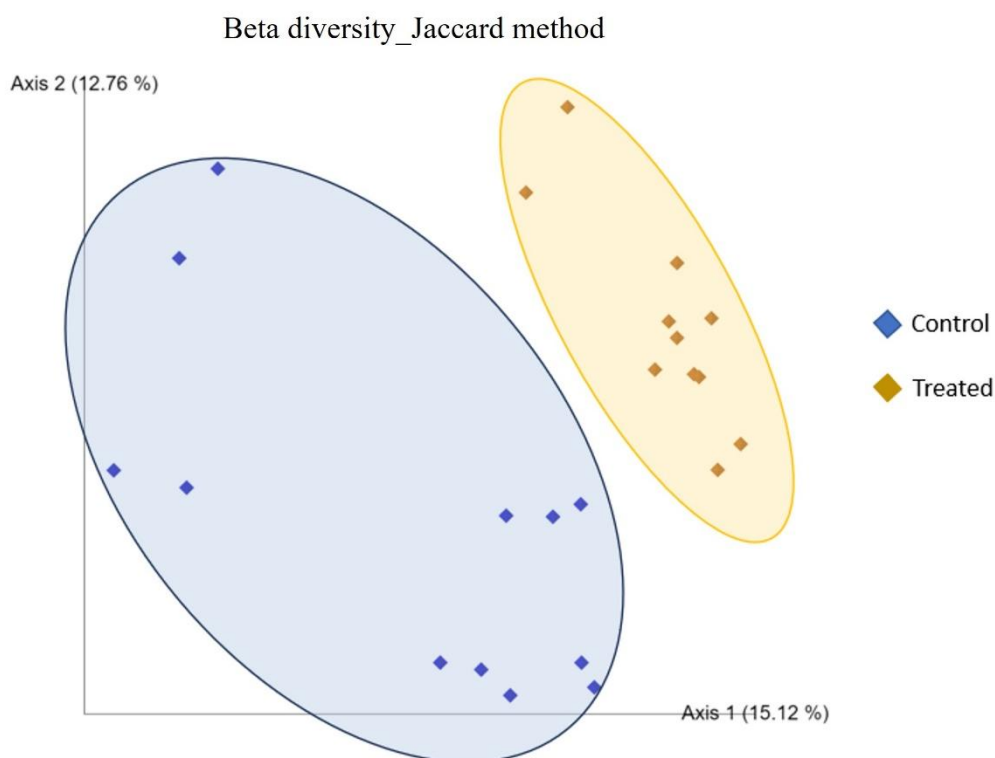
377 **Figure 5.** Taxonomic composition of the intestinal microbiota of *Hermetia illucens* at a) phylum level, b) family level,  
378 and c) genus level. Mean abundance was calculated for standard diet (control) (12 samples) and polystyrene diet (treated)  
379 (12 samples). Only bacteria taxa with an average relative abundance higher than 1% are reported.

380

381 The 16S rRNA gene sequencing evaluated the microbiota composition of BSF larvae fed with the PS-contaminated diet  
382 compared to the standard one. After only 2 weeks of feeding, the PS-containing substrate appeared to influence the  
383 composition of the intestinal bacterial community, compared to the control diet. At the phylum level, the PS-contaminated  
384 diet was predominantly composed of Firmicutes (46%), whereas in the control diet, the most abundant phyla were  
385 Proteobacteria (37.12%). On the family level, Actinomycetaceae exhibited similar abundance in the control and treated  
386 diets. However, Enterococcaceae was significantly more prevalent in the PS-contaminated diet, accounting for 38% of  
387 the total abundance. The Corynebacteriaceae family was present in the treated diet but absent in the control diet. At the  
388 genus level, the results were consistent; the PS-contaminated diet demonstrated a higher abundance of *Enterococcus*  
389 compared to the control, and the *Corynebacterium* genus was exclusively present in the PS-contaminated diet, comprising  
390 5.7% of the relative abundance. These findings suggest that these microbial genera may play a role in polystyrene  
391 degradation.

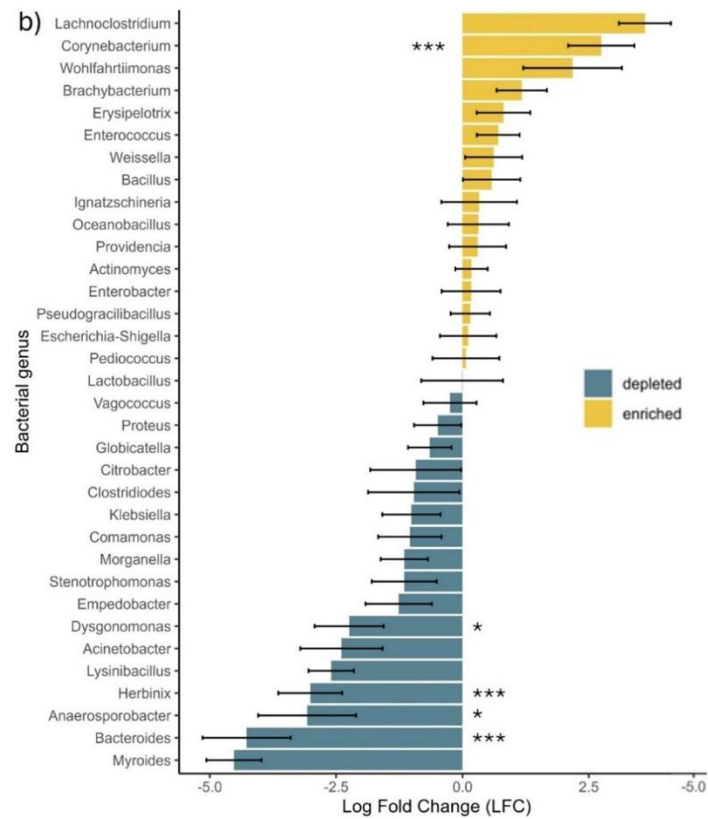
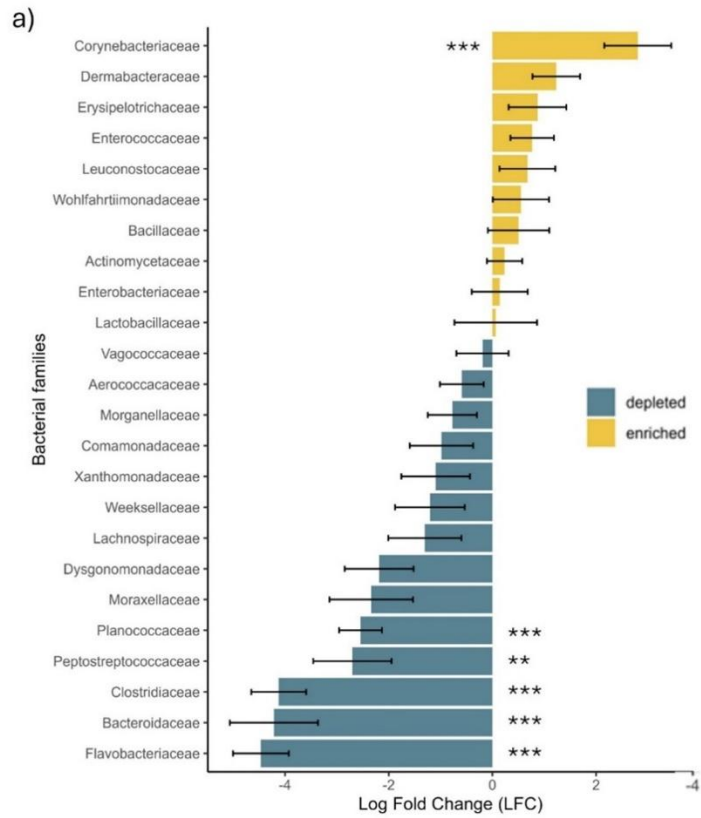
392 The alpha and beta diversity metrics were analysed using the respective QIIME2 plugins for both treatments. The alpha  
393 diversity indexes, Faith's phylogenetic diversity and Pielou evenness, indicated no significant differences in both diets  
394 (see **Figure S3**). The Kruskal-Wallis test confirmed no statistically significant differences between the control and treated  
395 diet groups for both the qualitative measure of community richness in terms of phylogenetic relationships (Faith-pd; H =  
396 3.18;  $p = 0.07$ ) and the measure of community distribution equity (Pielou-evenness; H = 2.18;  $p = 0.13$ ). These results  
397 suggest that neither treatment significantly affected the microbial communities' phylogenetic richness nor the distribution  
398 equity.

399 In contrast, beta diversity assessed by the Jaccard method and analysed with the PERMANOVA test showed a statistically  
400 significant difference ( $F = 3.05$ ;  $p < 0.001$ ) between the two treatment groups. This distinction is also visible in the PCoA  
401 graph for the Jaccard distance matrix (**Figure 6**), showing that the bacterial communities in the two treatments are  
402 dissimilar regarding their composition. This confirms the findings in **Figure 5 b** and **c**, which show different families and  
403 genera in the different treatments. This supports the hypothesis that the intestinal microbiota of the larvae fed on the PS-  
404 contaminated diet differs from that of the control diet due to the emergence of different microbial families and genera that  
405 can degrade the synthetic polymer.  
406



407  
408 **Figure 6.** Principal Co-ordinates Analysis (PCoA) for the Jaccard distance metrics. There is no overlap between the  
409 distribution of intestinal microbial communities of the control and treated larvae, indicating the diversity between the two  
410 bacterial communities. Blue= control diet (standard diet); yellow= treated diet (polystyrene diet).  
411

412 The PCoA plot showed a clear differentiation in the distribution of intestinal microbial communities between the two  
413 treatments, suggesting a relationship between microbial composition changes and polystyrene degradation; this is  
414 consistent with findings by De Filippis et al. (2023) and Wang et al. (2024). This distinction was further validated by  
415 examining the differential abundance of the various families and genera of bacteria found in both diets using ANCOM-  
416 BC (**Figure 7**).



419 **Figure 7.** Amplicon Sequence Variants are differentially abundant in the two treatments. The bars describe the relationship  
 420 between the treated group and the control group. Yellow bars represent the Amplicon Sequence Variants more abundantly  
 421 in the treated group. In contrast, blue bars represent the Amplicon Sequence Variants less abundantly in the treated group  
 422 compared to the control one. Thus, some Amplicon Sequence Variants are enriched (yellow) and depleted (blue) in the  
 423 treated group. The Amplicon Sequence Variants depleted in the treated group are enriched in the control group, and vice  
 424 versa. Graphs a) represent the family level, and b) represent the genus level. The asterisks indicate statistical significance:  
 425 \*\*\* maximum significance at 0.0001%, \*\* significance at 0.001%, \* significance at 0.05%. The bars indicate the standard  
 426 error (SE).  
 427

428 The differential abundance analyses revealed that the gut microbiota of BSF larvae fed with PS diet exhibited enrichment  
 429 in several bacteria families, including Corynebacteriaceae, Demabacteriaceae, Erysipelotrichaceae, Enterococaceae,  
 430 Leuconostocaceae, Wohlfahrtiimonadaceae, Bacillaceae, Actinomycetaceae, Enterobacteriaceae, and Lactobacteriaceae.  
 431 The family Corynebacteriaceae demonstrated a statistically significant differential abundance compared to the control  
 432 diet. Among the bacterial genera enriched in the PS-fed larvae, *Lachnoclostridium*, *Corynebacterium*, *Wohlfahrtiimonas*,  
 433 *Brachybacterium*, *Erysipelothrix*, *Enterococcus*, *Weissella*, *Bacillus*, *Ignatzschineria*, *Oceanobacillus*, *Providencia*,  
 434 *Actinomyces*, *Enterobacter*, *Pseudogracilibacillus*, *Escherichia-Shigella*, and *Pediococcus* were identified, with  
 435 *Corynebacterium* showing a particularly significant differential abundance. These findings are consistent with previous  
 436 studies by Sun et al. (2022) and Peydaei et al. (2021), which reported a substantial increase in the genus *Corynebacterium*  
 437 in larvae of *Z. atratus* and *G. mellonella* fed with PS diet. *Corynebacterium* is an aerobic bacterial genus known for its  
 438 involvement in the degradation pathway of polystyrene (Itoh et al., 1996; Itoh et al., 1997; Itch et al., 1997; O'Leary et  
 439 al., 2002; Mooney et al., 2006; Tischler, 2015; Danso et al., 2019). Specifically, *Corynebacterium* strains AC-5 and ST-5  
 440 can metabolise styrene via oxidation, converting it into styrene oxide and phenylacetaldehyde through the action of  
 441 styrene monooxygenase and styrene oxide isomerase enzymes (Itoh et al., 1996; O'Leary et al., 2002; Tischler, 2015;  
 442 Othman et al., 2021). This pathway was also observed by Sun et al. (2022), in which *Corynebacterium*, isolated from the  
 443 intestinal microbiota of *Z. atratus* larvae, degraded PS effectively using these enzymes. Our findings strongly suggest that  
 444 the exclusive presence of the genus *Corynebacterium* in the intestinal microbiota of PS-fed BSF larvae is closely  
 445 associated with the biodegradation of polystyrene microparticles.

446 In addition to *Corynebacterium*, other bacterial species such as *Pseudomonas putida*, *Xanthobacter*, *Rhodococcus*, *P.*  
 447 *fluorescens*, and *P. aeruginosa*, have been implicated in the polystyrene biodegradation pathway (Warhurst & Fewson,  
 448 1994; Itoh et al., 1996; Itoh et al., 1997; O'Leary et al., 2002; Mooney et al., 2006; Singh et al., 2012; Tischler, 2015;  
 449 Danso et al., 2021; Othman et al., 2021). Examination of the gut microbiota of PS-fed insect species revealed an increase  
 450 in bacteria associated with PS metabolism. For instance, Jiang et al. (2021) observed that *Enterococcus*,  
 451 *Enterobacteriaceae*, *Lactococcus*, *Enterobacter*, *Serratia*, and *Escherichia-Shigella* were favored in the gut microbiota  
 452 of *Z. atratus*, *G. mellonella*, and *T. molitor* subjected to a PS diet. Similarly, our results demonstrated an increase in  
 453 *Enterococcus*, *Enterobacteriaceae*, *Enterobacter*, and *Escherichia-Shigella* in the intestinal microbiota of PS-fed BSF  
 454 larvae.

455 Furthermore, studies on plastic-consuming insects, such as Urbanek et al. (2020), Jiang et al. (2021), Sun et al. (2022),  
 456 and De Filippis et al. (2023), have consistently reported an increase in the abundance of the phyla Actinobacteria and  
 457 Firmicutes when exposed to PS. These findings align with our results and suggest a potential correlation between these  
 458 phyla and their capacity to degrade or adapt to synthetic polymer-rich diets. Interestingly, despite the enrichment of  
 459 specific bacterial taxa, the total bacterial abundance in the PS-fed larvae was lower compared to the control diet. This  
 460 reduction could be attributed to developing chemical degradation by-products, such as styrene or styrene oligomers, which  
 461 may exert a bacteriostatic effect, as proposed by Tsochatzi et al. (2021).

462 Our findings highlight the potential of the intestinal microbiota of BSF larvae for isolating microbial strains optimised  
463 for plastic degradation. Investigating the microbial communities present in the gut of BSF larvae reared on synthetic  
464 polymers, such as PS, could facilitate the identification of enzymes with applications in plastic waste management. Recent  
465 studies on BSF larvae raised on diets contaminated with other microplastics, such as PVC, PP, and PE, have also suggested  
466 interactions between the gut microbiota and synthetic polymer degradation (Piersanti et al., 2024; Wang et al., 2024).  
467 However, further research is essential to elucidate the mechanisms by which BSF larvae contribute to the degradation of  
468 synthetic polymers, particularly polystyrene. Comprehensive investigations into the microbiota and enzymatic processes  
469 involved are crucial to understanding the role of BSF in polymer degradation and optimising its application in  
470 bioremediation strategies.

#### 471 **4. Conclusions**

472 The multidisciplinary investigation into the plastivorous activity of *H. illucens* larvae provides encouraging evidence of  
473 their capacity to degrade and bioconvert synthetic polymers, particularly polystyrene. The larval performance evaluation  
474 demonstrated remarkable adaptability, with no significant differences in growth performance or survival rates observed  
475 between larvae fed a PS-contaminated diet and those on a standard diet. These findings suggest that BSF larvae can utilise  
476 synthetic polymers as a carbon source and thrive in PS-rich environments. Ultrastructural observations through CLSM  
477 and TEM revealed the presence of PS microparticles primarily in the foregut and midgut, with minimal presence in the  
478 hindgut. Notably, fluorescence detected within the midgut epithelial cells suggests the translocation of PS by-products  
479 generated during microbial degradation. TEM analysis further confirmed dense aggregations of these by-products within  
480 the gut. Metagenomic analysis provided additional insights into the microbial communities associated with PS exposure.  
481 While we acknowledge that shift in gut microbiota composition can be influenced by a range of factors, our findings  
482 revealed changes compared to the control group that are consistent with those observed in other plastivorous insects.  
483 Specifically, the enrichment of *Corynebacterium* (a genus known for its role in aerobic PS degradation pathways) and the  
484 increased abundance of *Enterococcus*, *Enterobacteriaceae*, *Enterobacter*, and *Escherichia-Shigella* (bacterial taxa  
485 previously associated with plastic degradation), suggest a potential role in the bioconversion process. It is important to  
486 note that the PS microparticles used in this study were carboxylate-modified latex beads. Although these particles are  
487 widely used in laboratory settings as a model for polystyrene exposure, as previously reported, they differ from naturally  
488 occurring environmental microplastics, probably influencing microbial interactions or degradation dynamics. However,  
489 their use was essential in this and similar studies as their small size and aqueous dispersion made them the only viable  
490 option to ensure ingestion by *H. illucens* larvae, whose mouthparts are adapted to semi-liquid substrates. Moreover, their  
491 fluorescent properties enabled precise visualisation during ultrastructural observations.

492 This study strengthens the hypothesis that BSF larvae contribute to plastic waste degradation, elucidates some  
493 mechanisms underlying this process, and provides a valuable foundation for future research on insect-mediated polymer  
494 degradation. Future studies should focus on isolating and cultivating the bacterial communities involved and elucidating  
495 the enzymatic pathways driving PS biodegradation. These investigations will enhance the understanding of BSF larvae's  
496 potential in sustainable waste management applications, offering a promising strategy to address the global challenge of  
497 plastic pollution.

498

499

#### 500 **References**

501 Adamaki-Sotiraki C, Abenaim L, Mannucci A, Rumbos CI, Bedini S, Castagna A, Conte G, Tognocchi M, Dolianitis  
502 V, Athanassiou CG, Conti B (2024) Performance of *Hermetia illucens* (Diptera: Stratiomyidae) larvae reared on  
503 organic waste diets and pupal chitin and chitosan yield. *ESPR*, 1-10. <https://doi.org/10.1007/s11356-024-33545-x>

504 Amrul NF, Kabir Ahmad I, Ahmad Basri NE, Suja F, Abdul Jalil NA, Azman NA (2022) A review of organic waste  
505 treatment using black soldier fly (*Hermetia illucens*). *Sustainability*, 14(8), 4565. <https://doi.org/10.3390/su14084565>

506 Arunrattiyakorn P, Ponprateep S, Kaennonsang N, Charapok Y, Punphuet Y, Krajangsang S, Tangteerawatana P,  
507 Limtrakul A (2022) Biodegradation of polystyrene by three bacterial strains isolated from the gut of Superworms  
508 (*Zophobas atratus* larvae). *J. Appl. Microbiol.*, 132(4), 2823-2831. <https://doi.org/10.1111/jam.15474>

509 Block C, Brands B, Gude T (2017) *Packaging Materials 2. Polystyrene for Food Packaging Applications—Updated*  
510 *Version. International Life Sciences Institute.*

511 Bokulich NA, Dillon MR, Bolyen E, Kaehler BD, Huttley GA, Caporaso JG (2018) Q2-sample-classifier: machine-  
512 learning tools for microbiome classification and regression. *JORS*, 3(30). <https://doi.org/10.21105/joss.00934>

513 Bolyen E, Rideout JR, Dillon MR, Bokulich NA, Abnet CC, Al-Ghalith GA, Alexander H, Alm EJ, Arumugam M,  
514 Asnica F, Bai Y, Bisanz JE, Bittinger K, Brehnerod A, Brislawn CJ, Brown TC, Callahan BJ, Caraballo-Rodriguez  
515 AM, Chase J, Cope EK, De Silva R, Diener C, Dorrestein PC, Douglas GM, et al. Caporaso JG (2019) Reproducible,  
516 interactive, scalable and extensible microbiome data science using QIIME 2. *Nat. biotechnol.*, 37(8), 852-857.

517 Brandon AM, Gao SH, Tian R, Ning D, Yang SS, Zhou J, Wu WM, Criddle CS (2018) Biodegradation of polyethylene  
518 and plastic mixtures in mealworms (larvae of *Tenebrio molitor*) and effects on the gut microbiome. *Environ. Sci.*  
519 *Technol.*, 52(11), 6526-6533. <https://doi.org/10.1021/acs.est.8b02301>

520 Bruno D, Bonelli M, De Filippis F, Di Lelio I, Tettamanti G, Casartelli M, Ercolini D, Caccia S (2019) The intestinal  
521 microbiota of *Hermetia illucens* larvae is affected by diet and shows a diverse composition in the different midgut  
522 regions. *Appl. Environ. Microbiol.*, 85(2), e01864-18. <https://doi.org/10.1128/AEM.01864-18>

523 Bulak P, Polakowski C, Nowak K, Waśko A, Wiącek D, Bieganski A (2018) *Hermetia illucens* as a new and  
524 promising species for use in entomoremediation. *Sci. Total Environ.*, 633, 912-919.  
525 <https://doi.org/10.1016/j.scitotenv.2018.03.252>

526 Callahan BJ, McMurdie PJ, Rosen MJ, Han AW, Johnson AJA., Holmes SP (2016) DADA2: High-resolution sample  
527 inference from Illumina amplicon data. *Nat. Methods*, 13(7), 581-583. <https://doi.org/10.1038/nmeth.3869>

528 Camenzuli L, Van Dam R, De Rijk T, Andriessen R, Van Schelt J, der Fels-Klerx V (2018) Tolerance and excretion  
529 of the mycotoxins aflatoxin B1, zearalenone, deoxynivalenol, and ochratoxin A by *Alphitobius diaperinus* and  
530 *Hermetia illucens* from contaminated substrates. *Toxins*, 10(2), 91. <https://doi.org/10.3390/toxins10020091>

531 Carpentier J, Abenaim L, Luttenschlager H, Dessauvages K, Liu Y, Samoah P, Francis F, Caparros Megido R (2024)  
532 Microorganism Contribution to Mass-Reared Edible Insects: Opportunities and Challenges. *Insects*, 15(8), 611.  
533 <https://doi.org/10.3390/insects15080611>

534 Cho S, Kim CH, Kim MJ, Chung H (2020) Effects of microplastics and salinity on food waste processing by black  
535 soldier fly (*Hermetia illucens*) larvae. *J. Ecol. Environ.*, 44(1), 1-9. <https://doi.org/10.1186/s41610-020-0148-x>

536 Cucini C, Leo C, Vitale M, Frati F, Carapelli A, Nardi F (2020) Bacterial and fungal diversity in the gut of  
537 polystyrene-fed *Alphitobius diaperinus* (Insecta: Coleoptera). *Animal Gene*, 17, 200109.  
538 <https://doi.org/10.1016/j.angen.2020.200109>

539 Danso D, Chow J, Streit WR (2019) Plastics: environmental and biotechnological perspectives on microbial  
540 degradation. *Appl. Environ. Microbiol.*, 85(19), e01095-19. <https://doi.org/10.1128/AEM.01095-19>

541 De Filippis F, Bonelli M, Bruno D, Sequino G, Montali A, Reguzzoni M, Pasolli E, Savy D, Cangemi S, Cozzolino  
542 V, Tattamanti G, Ercolini D, Caccia S (2023) Plastics shape the black soldier fly larvae gut microbiome and select  
543 for biodegrading functions. *Microbiome*, 11(1), 205. <https://doi.org/10.1186/s40168-023-01649-0>

544 De Smet J, Wynants E, Cos P, Van Campenhout L (2018) Microbial community dynamics during rearing of black  
545 soldier fly larvae (*Hermetia illucens*) and impact on exploitation potential. *Appl. Environ. Microbiol*, 84(9), e02722-  
546 17. <https://doi.org/10.1128/AEM.02722-17>

547 El Kholy S, Al Naggari Y (2023) Exposure to polystyrene microplastic beads causes sex-specific toxic effects in the  
548 model insect *Drosophila melanogaster*. *Scientific Reports*, 13(1), 204. <https://doi.org/10.1038/s41598-022-27284-7>

549 Elmekawy A, Elshehaby M, Saber S, Ayaad T (2023). Evaluation of *Galleria mellonella* immune response as a key  
550 step toward plastic degradation. *JOBAZ*, 84(1), 27. <https://doi.org/10.1186/s41936-023-00349-3>

551 Engel P, Moran NA (2013) The gut microbiota of insects—diversity in structure and function. *FEMS Microbiol.*  
552 *Rev.*, 37(5), 699-735. <https://doi.org/10.1111/1574-6976.12025>

553 Europe P (2024) *The circular economy for plastics: a European overview, 2022.*  
554 <https://plasticseurope.org/knowledge-hub/the-circular-economy-for-plastics-a-european-analysis-2024/> (Accessed  
555 February 2025)

556 Fuller S, Gautam A (2016) A procedure for measuring microplastics using pressurized fluid  
557 extraction. *Environmental science & technology*, 50(11), 5774-5780.  
558 <https://pubs.acs.org/doi/abs/10.1021/acs.est.6b00816>

559 Heussler CD, Dittmann IL, Egger B, Robra S, Klammsteiner T (2024) A Comparative Study of Effects of  
560 Biodegradable and Non-biodegradable Microplastics on the Growth and Development of Black Soldier Fly Larvae  
561 (*Hermetia illucens*). *Waste and Biomass Valorization*, 15(4), 2313-2322. <https://doi.org/10.1007/s12649-023-02296-0>

562

563 Ho BT, Roberts TK, Lucas S (2018) An overview on biodegradation of polystyrene and modified polystyrene: the  
564 microbial approach. *Critical reviews in biotechnology*, 38(2), 308-320.  
565 <https://doi.org/10.1080/07388551.2017.1355293>

566 Hou L, Majumder ELW (2021) Potential for and distribution of enzymatic biodegradation of polystyrene by  
567 environmental microorganisms. *Materials*, 14(3), 503. <https://doi.org/10.3390/ma14030503>

568 Itch N, Hayashi K, Okada K, Ito T, Mizuguchi N (1997) Characterization of Styrene Oxide Isomerase, a Key Enzyme  
569 of Styrene and Styrene Oxide Metabolism in *Corynebacterium* sp. *Biosci., Biotechnol., Biochem.*, 61(12), 2058-  
570 2062. <https://doi.org/10.1271/bbb.61.2058>

571 Itoh N, Morihama R, Wang J, Okada K, Mizuguchi N (1997) Purification and characterization of phenylacetaldehyde  
572 reductase from a styrene-assimilating *Corynebacterium* strain, ST-10. Appl. Environ. Microbiol., 63(10), 3783-3788.  
573 <https://doi.org/10.1128/aem.63.10.3783-3788.1997>

574 Itoh N, Yoshida K, Okada K (1996) Isolation and identification of styrene-degrading *Corynebacterium* strains, and  
575 their styrene metabolism. Biosci., Biotechnol., Biochem., 60(11), 1826-1830. <https://doi.org/10.1271/bbb.60.1826>

576 Jiang S, Su T, Zhao J, Wang Z (2021) Biodegradation of polystyrene by *Tenebrio molitor*, *Galleria mellonella*, and  
577 *Zophobas atratus* larvae and comparison of their degradation effects. Polymers, 13(20), 3539.  
578 <https://doi.org/10.3390/polym13203539>

579 Kaczor M, Bulak P, Proc-Pietrycha K, Kirichenko-Babko M, Bieganski A (2022) The variety of applications of  
580 *Hermetia illucens* in industrial and agricultural areas. Biology, 12(1), 25. <https://doi.org/10.3390/biology12010025>

581 Klindworth A, Pruesse E, Schweer T, Peplies J, Quast C, Horn M, Glöckner FO (2013) Evaluation of general 16S  
582 ribosomal RNA gene PCR primers for classical and next-generation sequencing-based diversity studies. Nucleic  
583 acids research, 41(1), e1-e1. <https://doi.org/10.1093/nar/gks808>

584 Koga R, Tsuchida T, Fukatsu T (2009) Quenching autofluorescence of insect tissues for in situ detection of  
585 endosymbionts. Appl. Entomol. Zool., 44(2), 281-291. <https://doi.org/10.1303/aez.2009.281>

586 Kuan ZJ, Chan BKN, Gan SKE (2022) Worming the circular economy for biowaste and plastics: *Hermetia illucens*,  
587 *Tenebrio molitor*, and *Zophobas morio*. Sustainability, 14(3), 1594. <https://doi.org/10.3390/su14031594>

588 Lievens S, Poma G, Frooninckx L, Van der Donck T, Seo JW, De Smet J, Covaci A, Van Der Borgh M (2022) Mutual  
589 influence between polyvinyl chloride (micro) plastics and black soldier fly larvae (*Hermetia illucens* L.).  
590 Sustainability, 14(19), 12109. <https://doi.org/10.3390/su141912109>

591 Lin H, Peddada SD (2020) Analysis of compositions of microbiomes with bias correction. Nat. Commun., 11(1),  
592 3514. <https://doi.org/10.1038/s41467-020-17041-7>

593 Liu C, Yao H, Chapman SJ, Su J, Wang C (2020) Changes in gut bacterial communities and the incidence of antibiotic  
594 resistance genes during degradation of antibiotics by black soldier fly larvae. Environ. Int., 142, 105834.  
595 <https://doi.org/10.1016/j.envint.2020.105834>

596 Lou Y, Ekaterina P, Yang SS, Lu B, Liu B, Ren N, Corvini PE, Xing D (2020) Biodegradation of polyethylene and  
597 polystyrene by greater wax moth larvae (*Galleria mellonella* L.) and the effect of co-diet supplementation on the  
598 core gut microbiome. Environ. Sci. Technol., 54(5), 2821-2831. <https://doi.org/10.1021/acs.est.9b07044>

599 Martin M (2011) Cutadapt removes adapter sequences from high-throughput sequencing reads. EMBnet. journal,  
600 17(1), 10-12. <https://doi.org/10.14806/ej.17.1.200>

601 Matyja K, Rybak J, Hanus-Lorenz B, Wróbel M, Rutkowski R (2020) Effects of polystyrene diet on *Tenebrio molitor*  
602 larval growth, development and survival: Dynamic Energy Budget (DEB) model analysis. Environ. Pollut., 264,  
603 114740. <https://doi.org/10.1016/j.envpol.2020.114740>

604 Mei H, Li C, Li X, Hu B, Lu L, Tomberlin JK, Hu W (2022) Characteristics of tylosin and enrofloxacin degradation  
605 in swine manure digested by black soldier fly (*Hermetia illucens* L.) larvae. Environ. Pollut., 293, 118495.  
606 <https://doi.org/10.1016/j.envpol.2021.118495>

607 Monici M (2005) Cell and tissue autofluorescence research and diagnostic applications. *Biotechnol. Annu. Rev.* 11,  
608 227-256. [https://doi.org/10.1016/S1387-2656\(05\)11007-2](https://doi.org/10.1016/S1387-2656(05)11007-2)

609 Mooney A, Ward PG, O'Connor KE (2006) Microbial degradation of styrene: biochemistry, molecular genetics, and  
610 perspectives for biotechnological applications. *AMBB*, 72, 1-10. <https://doi.org/10.1007/s00253-006-0443-1>

611 Muhammad A, Zhou X, He J, Zhang N, Shen X, Sun C, Yan B, Shao, Y. (2021). Toxic effects of acute exposure to  
612 polystyrene microplastics and nanoplastics on the model insect, silkworm *Bombyx mori*. *Environ. Pollut.*, 285,  
613 117255. <https://doi.org/10.1016/j.envpol.2021.117255>

614 Noël G, Serteyn L, Sare AR, Massart S, Delvigne F, Francis F (2023) Co-diet supplementation of low density  
615 polyethylene and honeybee wax did not influence the core gut bacteria and associated enzymes of *Galleria mellonella*  
616 larvae (Lepidoptera: Pyralidae). *International Microbiology*, 26(2), 397-409. <https://doi.org/10.1007/s10123-022-00303-3>

617

618 Nyakeri EM, Ogola HJO, Ayieko MA, Amimo FA (2017) Valorisation of organic waste material: growth performance  
619 of wild black soldier fly larvae (*Hermetia illucens*) reared on different organic wastes. *JIFF*, 3(3), 193-202.  
620 <https://doi.org/10.3920/JIFF2017.0004>

621 O'Leary ND, O'Connor KE, Dobson AD (2002) Biochemistry, genetics and physiology of microbial styrene  
622 degradation. *FEMS microbiology reviews*, 26(4), 403-417. <https://doi.org/10.1111/j.1574-6976.2002.tb00622.x>

623 Othman AR, Hasan HA, Muhamad MH, Ismail NI, Abdullah SRS (2021) Microbial degradation of microplastics by  
624 enzymatic processes: a review. *Environ. Chem. Lett.*, 19, 3057-3073. <https://doi.org/10.1007/s10311-021-01197-9>

625 Pena-Pascagaza PM, Lopez-Ramirez NA, Ballen-Segura MA (2020) *Tenebrio molitor* and its gut bacteria growth in  
626 polystyrene (PS) presence as the sole source carbon. *Universitas Scientiarum*, 25(1), 37-53.  
627 <https://doi.org/10.11144/Javeriana.SC25-1.tmaj>

628 Peng BY, Li Y, Fan R, Chen Z, Chen J, Brandon AM, Craig SC, Zhang Y, Wu WM (2020) Biodegradation of low-  
629 density polyethylene and polystyrene in superworms, larvae of *Zophobas atratus* (Coleoptera: Tenebrionidae): Broad  
630 and limited extent depolymerization. *Environ. Pollut.*, 266, 115206. <https://doi.org/10.1016/j.envpol.2020.115206>

631 Peng BY, Sun Y, Wu Z, Chen J, Shen Z, Zhou X, Wei-Min W, Zhang Y (2022) Biodegradation of polystyrene and  
632 low-density polyethylene by *Zophobas atratus* larvae: Fragmentation into microplastics, gut microbiota shift, and  
633 microbial functional enzymes. *J. Clean. Prod.*, 367, 132987. <https://doi.org/10.1016/j.jclepro.2022.132987>

634 Peydaei A, Bagheri H, Gurevich L, de Jonge N, Nielsen JL (2021) Mastication of polyolefins alters the microbial  
635 composition in *Galleria mellonella*. *Environ. Pollut.*, 280, 116877. <https://doi.org/10.1016/j.envpol.2021.116877>

636 Piersanti S, Rebori M, Turchettwang B, Salerno G, Ruscetta M, Zucconi L, D'Alò F, Buzzini P, Sannino C (2024)  
637 Microplastics in the diet of *Hermetia illucens*: Implications for development and midgut bacterial and fungal  
638 microbiota. *Waste Management*, 186, 259-270. <https://doi.org/10.1016/j.wasman.2024.06.021>

639 Pivato AF, Miranda GM, Prichula J, Lima JE, Ligabue RA, Seixas A, Trentin DS (2022) Hydrocarbon-based plastics:  
640 Progress and perspectives on consumption and biodegradation by insect larvae. *Chemosphere*, 133600.  
641 <https://doi.org/10.1016/j.chemosphere.2022.133600>

642 Porterfield KK, Hobson SA, Neher DA, Niles MT, Roy ED (2023) Microplastics in composts, digestates, and food  
643 wastes: A review. *Journal of Environmental Quality*, 52(2), 225-240. <https://doi.org/10.1002/jeq2.20450>

644 Prabhakar N, Peurla M, Shenderova O, Rosenholm JM (2020) Fluorescent and electron-dense green color emitting  
645 nanodiamonds for single-cell correlative microscopy. *Molecules*, 25(24), 5897.  
646 <https://doi.org/10.3390/molecules25245897>

647 Quan Z, Zhao Z, Liu Z, Wang W, Yao S, Liu H, Lin X, Li QX, Yan H, Liu X (2023) Biodegradation of polystyrene  
648 microplastics by superworms (larve of *Zophobas atratus*): Gut microbiota transition, and putative metabolic  
649 ways. *Chemosphere*, 343, 140246. <https://doi.org/10.1016/j.chemosphere.2023.140246>

650 Robeson MS, O'Rourke DR, Kaehler BD, Ziemski M, Dillon MR, Foster JT, Bokulich NA (2021) RESCRIPT:  
651 Reproducible sequence taxonomy reference database management. *PLoS Comput. Biol.*, 17(11), e1009581.  
652 <https://doi.org/10.1371/journal.pcbi.1009581>

653 Romano N, Fischer H (2021) Microplastics affected black soldier fly (*Hermetia illucens*) pupation and short chain  
654 fatty acids. *J. Appl. Entomol.*, 145(7), 731-736. <https://doi.org/10.1111/jen.12887>

655 Ru J, Huo Y, Yang Y (2020) Microbial degradation and valorization of plastic wastes. *Frontiers in Microbiology*, 11,  
656 442. <https://doi.org/10.3389/fmicb.2020.00442>

657 Sanchez-Hernandez JC (2021) A toxicological perspective of plastic biodegradation by insect larvae. *CBP Part C:  
658 Toxicology & Pharmacology*, 248, 109117. <https://doi.org/10.1016/j.cbpc.2021.109117>

659 Singh SN, Kumari B, Mishra S (2012) Microbial degradation of alkanes. *Microbial degradation of xenobiotics*, 439-  
660 469. [https://doi.org/10.1007/978-3-642-23789-8\\_17](https://doi.org/10.1007/978-3-642-23789-8_17)

661 Sun J, Prabhu A, Aroney ST, Rinke C (2022) Insights into plastic biodegradation: community composition and  
662 functional capabilities of the superworm (*Zophobas morio*) microbiome in styrofoam feeding trials. *Microb.  
663 Genom.*, 8(6). <https://doi.org/10.1099/mgen.0.000842>

664 Suo J, Liang T, Zhang H, Liu K, Li X, Xu K, Guo J, Luo Q, Yang S (2023) Characteristics of Aflatoxin B1  
665 Degradation by *Stenotrophomonas acidaminiphila* and It's Combination with Black Soldier Fly Larvae. *Life*, 13(1),  
666 234. <https://doi.org/10.3390/life13010234>

667 Tischler D (2015) *Microbial styrene degradation* (No. 11725). Cham, Switzerland: Springer International Publishing.  
668 <https://doi.org/10.1007/978-3-319-24862-2>

669 Tsochatzis E, Berggreen IE, Tedeschi F, Ntrallou K, Gika H, Corredig M (2021) Gut microbiome and degradation  
670 product formation during biodegradation of expanded polystyrene by mealworm larvae under different feeding  
671 strategies. *Molecules*, 26(24), 7568. <https://doi.org/10.3390/molecules26247568>

672 Tsochatzis E, Lopes JA, Gika H, Theodoridis G (2020) Polystyrene biodegradation by *Tenebrio molitor* larvae:  
673 identification of generated substances using a GC-MS untargeted screening method. *Polymers*, 13(1), 17.  
674 <https://doi.org/10.3390/polym13010017>

675 Ullah R, Tsui MTK, Chow A, Chen H, Williams C, Ligaba-Osena A (2023) Micro (nano) plastic pollution in  
676 terrestrial ecosystem: emphasis on impacts of polystyrene on soil biota, plants, animals, and humans. *Environ. Monit.  
677 Assess.*, 195(1), 252. <https://doi.org/10.1007/s10661-022-10769-3>

678 Urbanek AK, Rybak J, Wróbel M, Leluk K, Mirończuk AM (2020) A comprehensive assessment of microbiome  
679 diversity in *Tenebrio molitor* fed with polystyrene waste. *Environ. Pollut.*, 262, 114281.  
680 <https://doi.org/10.1016/j.envpol.2020.114281>

681 Wang J, Liu C, Cao Q, Li Y, Chen L, Qin Y, Wang T, Wang C (2024) Enhanced biodegradation of microplastic and  
682 phthalic acid ester plasticizer: The role of gut microorganisms in black soldier fly larvae. *Sci. Total Environ.*, 924,  
683 171674. <https://doi.org/10.1016/j.scitotenv.2024.171674>

684 Wang K, Li J, Zhao L, Mu X, Wang C, Wang M, Xue X, Qi S, Wu L (2021) Gut microbiota protects honeybees (*Apis*  
685 *mellifera* L.) against polystyrene microplastics exposure risks. *J. Hazard. Mater.*, 402, 123828.  
686 <https://doi.org/10.1016/j.jhazmat.2020.123828>

687 Wang S, Shi W, Huang Z, Zhou N, Xie Y, Tang Y, Hu F, Liu G, Zheng H (2022) Complete digestion/biodegradation  
688 of polystyrene microplastics by greater wax moth (*Galleria mellonella*) larvae: Direct in vivo evidence, gut  
689 microbiota independence, and potential metabolic pathways. *J. Hazard. Mater.*, 423, 127213.  
690 <https://doi.org/10.1016/j.jhazmat.2021.127213>

691 Warhurst AM, Fewson CA (1994) Microbial metabolism and biotransformations of styrene. *J. Appl. Bacteriol.*, 77(6),  
692 597-606.

693 Yang Y, Wang J, Xia M (2020) Biodegradation and mineralization of polystyrene by plastic-eating superworms  
694 *Zophobas atratus*. *Sci. Total Environ.*, 708, 135233. <https://doi.org/10.1016/j.scitotenv.2019.135233>

695

696 **Author contributions: Conceptualisation:** Abenaim Linda; Investigation: Abenaim Linda, Mercati David, Mandoli  
697 Alessandro; **Methodology:** Abenaim Linda, Mercati David, Mandoli Alessandro, Carpentier Joachim, Noël Grégoire;  
698 **Data curation:** Abenaim Linda; Formal analysis: Abenaim Linda, **Writing-original draft preparation:** Abenaim Linda;  
699 **Writing- review and editing:** Abenaim Linda, Mercati David, Mandoli Alessandro, Carpentier Joachim, Noël Grégoire,  
700 Conti Barbara, Caparros Megido Rudy, Dallai Romano; **Supervision:** Conti Barbara, Caparros Megido Rudy, Dallai  
701 Romano; **Funding acquisition:** Conti Barbara, Caparros Megido Rudy, Dallai Romano.

702

703 **Declaration of competing interest:** The authors have no relevant financial or non-financial interests to disclose.

704

705 **Funding:** The authors declare that no funds, grants, or other support were received during the preparation of this  
706 manuscript.

707

708 **Acknowledgement:** Computational resources have been provided by the Consortium des Équipements de Calcul Intensif  
709 (CÉCI), funded by the Fonds de la Recherche Scientifique de Belgique (F.R.S.-FNRS) under Grant No. 2.5020.11 and by  
710 the Walloon Region.

711

712 **Ethical Approval:** Not applicable

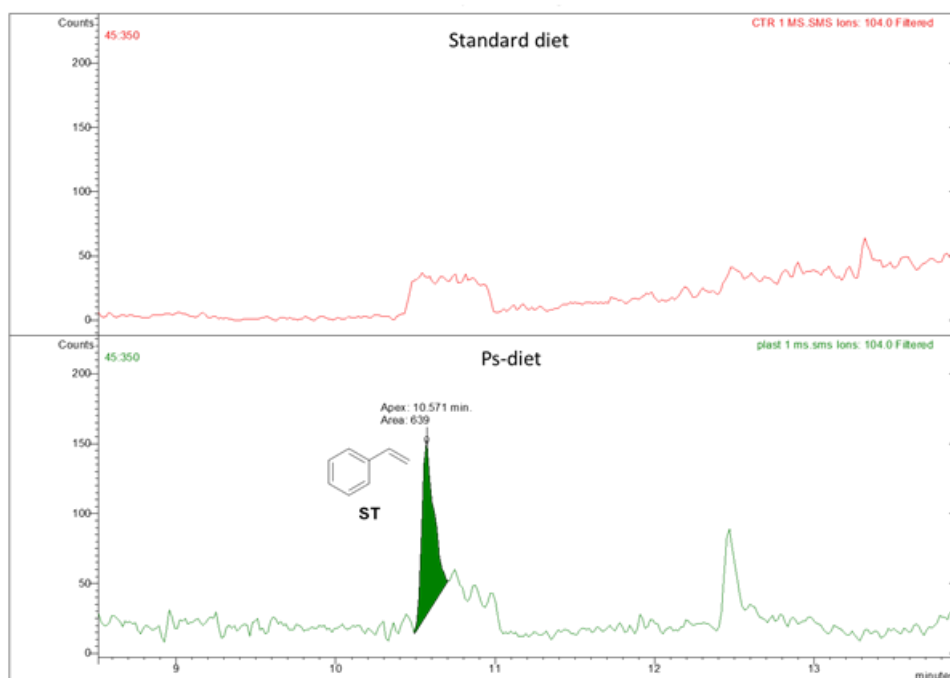
713 **Consent to Participate:** Not applicable

714 **Consent to Publish:** Not applicable

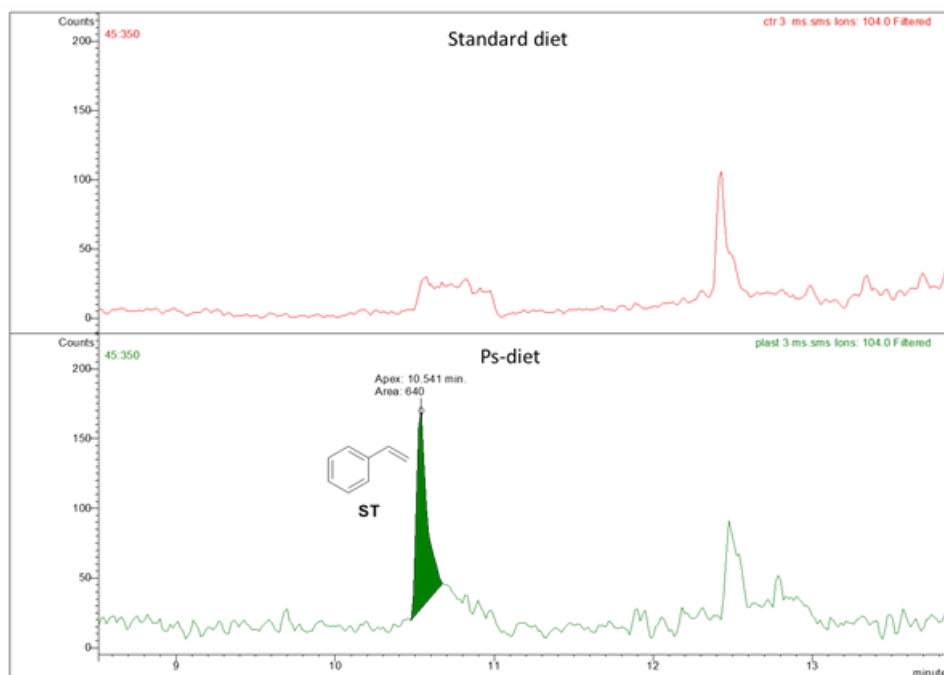
715 **Data availability statement:** data are available upon request to the corresponding author.



## a) Chromatogram plot 1 day of feeding

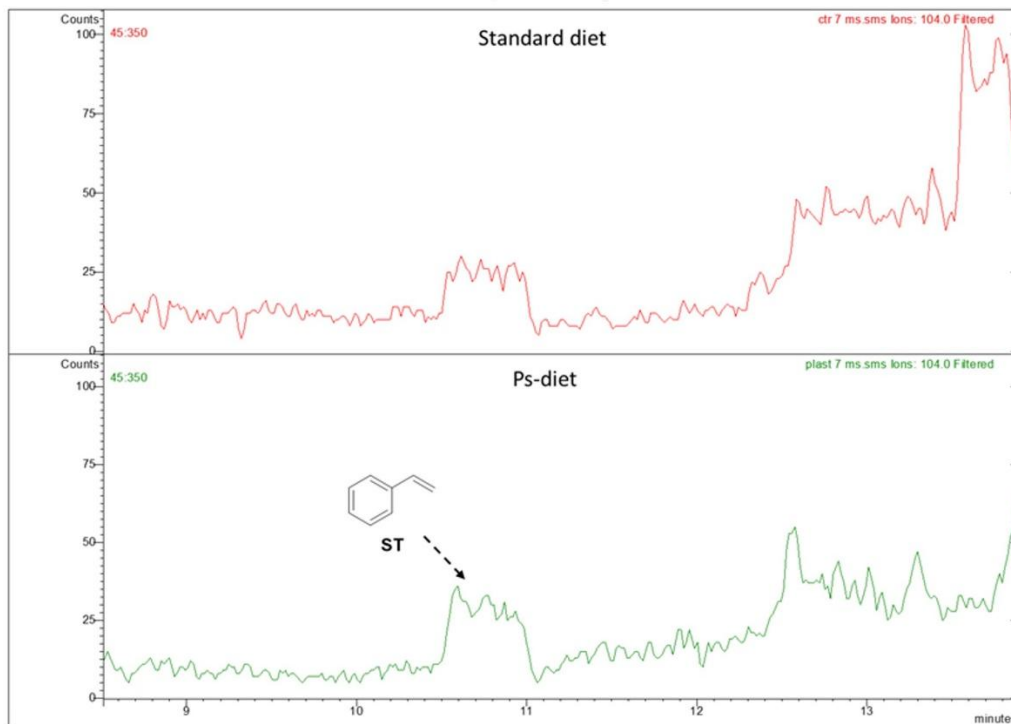


## b) Chromatogram plot 3 days of feeding



720 **Figure S2 a, b.** Chromatogram plot extracted with Gas Chromatography-Mass Spectrometry of the lyophilised intestines  
721 of Black Soldier Fly larvae, after 1 day (a) and 3 days (b) of feeding. The red spectrum represents the control (standard  
722 diet), and the green spectrum represents the treated (polystyrene diet).  
723

Chromatogram plot 7 days of feeding

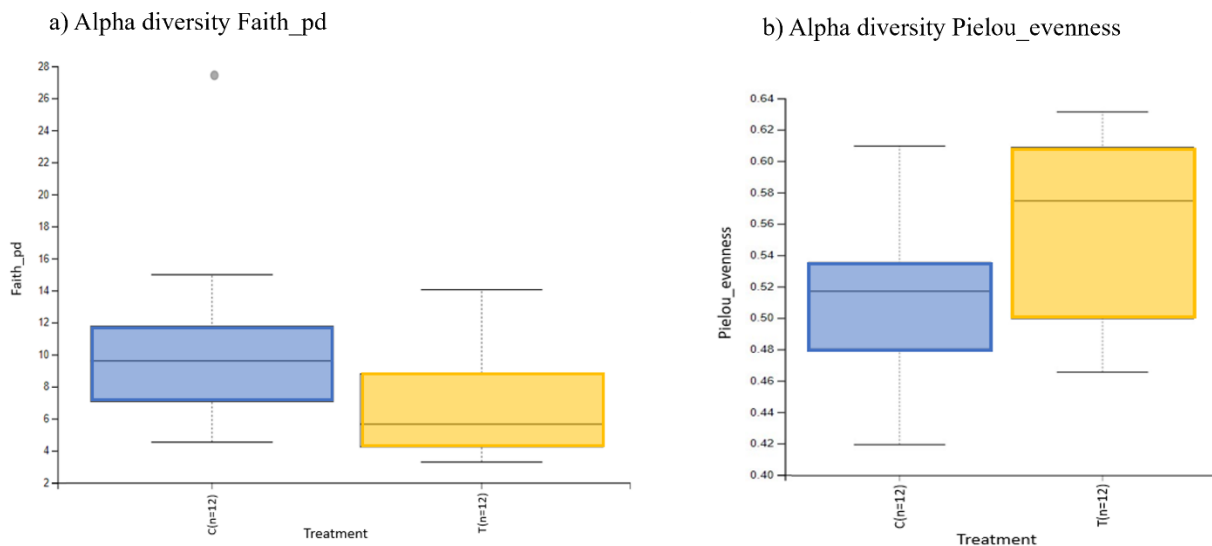


724

725 **Figure S2.** Chromatogram plot extracted with Gas Chromatography-Mass Spectrometry of the lyophilised intestines of  
 726 Black Soldier Fly larvae, after 7 days of PS feeding. The red spectrum represents the control (standard diet), and the green  
 727 spectrum represents the treated (polystyrene diet).  
 728

728

729



730

731

732 **Figure S3 a, b.** The Kruskal-Wallis significance boxplot for alpha diversity metrics is based on the treatment factor  
 733 (control diet and treated diet). The boxplots indicate no difference in alpha diversity between the bacteria in the two  
 734 treatments ( $p > 0.05$ ). a) alpha diversity based on Faith-pd, b) alpha diversity based on Pielou-evenness. For both diversity  
 735 12 samples per treatment were analysed.  
 736

736